Laboratory Experiments on Cometary Materials

L. Colangeli and J. R. Brucato
Istituto Nazionale di Astrofisica–Osservatorio Astronomico di Capodimonte

A. Bar-Nun
Tel Aviv University

R. L. Hudson
Eckerd College and NASA Goddard Space Flight Center

M. H. Moore
NASA Goddard Space Flight Center

Laboratory experiments to simulate cometary materials and their processing contribute to the investigation of the properties and evolution of comets. Experimental methods can produce both refractory materials and frozen volatiles with chemical, structural, and morphological characteristics that reproduce those of materials observed and/or expected in comets. Systematic analyses of such samples, before and after energetic processing by various agents effective in the solar system, provide a wealth of useful quantitative information. Such data permit a more complete interpretation of observations, performed remotely or *in situ*, and suggest ideas about the chemical and physical evolution of cometary dust and ice. Finally, laboratory results help to predict the environmental conditions that future space missions, such as the European Space Agency's *Rosetta* mission, will experience, and thus aid in properly planning mission and instrument development.

1. INTRODUCTION

Comets are considered to be reservoirs of partially uncontaminated primordial material from which the solar system formed about 4.5×10^9 yr ago. The composition as well as the physical and structural properties of cometary dust and ice depend both on comet formation mechanisms and postaccretion evolutionary processes. The so-called "interstellar grain" model (e.g., *Greenberg and Hage,* 1990; *Mumma,* 1997; *Notesco et al.,* 2003) supports the concept that comets formed far (>20 AU) from the proto-Sun, at low temperatures (<100 K or so), so that their composition should reflect that of original interstellar cloud grains. In contrast, the "nebular chemistry" model includes the possibility that interstellar material may have been reprocessed prior to cometary formation (e.g., *Lunine,* 1989). The resulting cometary chemistry is different in these two scenarios, mainly due to the ice condensation temperature. However, it is possible that cometary chemistry reflects both the presence of original interstellar grains and reprocessed materials (*Engel et al.,* 1990). Details about comet formation and evolution are described by *Dones et al.* (2004).

The internal structure of comets also depends on the dynamic evolution of the protosolar nebula. As settling toward the midplane of the nebula occurred, did infalling material collapse into kilometer-sized planetesimals (*Goldreich and Ward,* 1973), or did it accumulate into 50–100-m aggregates (*Weidenschilling,* 1997)? The "rubble pile" model would be acceptable in the first case (*Weissman,* 1986), but a different preferred size scale should exist in the latter [see *Weissman et al.* (2004) for more details about comet nuclear structure].

The exploration of Comet 1P/Halley provided a breakthrough in the understanding of cometary structure and composition, thanks to close observations of Halley's nucleus (see *Keller et al.,* 2004). More recently, remote observations, such as with the Infrared Space Observatory (ISO), have provided valuable insights into cometary chemistry. Major progress has concerned the identification of a large variety of volatile molecules (*Bockelée-Morvan et al.,* 2004) and a deeper characterization of the refractory components of cometary and interstellar dust, especially silicates (*Hanner and Bradley,* 2004). This new information has allowed us to forge strong links between comet composition and interstellar dust evolution (*Ehrenfreund et al.,* 2004).

Even with such new observations, uncertainties remain concerning the properties and evolution of materials that form comets. Laboratory experiments now play a fundamental role in research programs designed to reveal the main components of comets and the effects of energetic processing experienced by cometary ice and dust. The experimental program applied to ice and dust investigations is based on three main steps: (1) production of materials by techniques that allow control of product characteristics; (2) analyses of dust and ice analogs by complementary methods aimed at quantitative studies of morphology, structure, chemistry, and optical behavior; and (3) processing to

reproduce effects expected in space before, during, and after comet formation.

The results of such experiments are extremely useful for quantitative interpretation of astronomical observations. By studying dust and ice properties as a function of formation conditions and levels of energetic processing, light can be shed on the formation and evolution of materials in the solar system in general and comets in particular. This approach not only complements observations, but it has predictive power for observers and provides important constraints for theoretical models.

This chapter provides an overview of past and ongoing experimental work. Section 2 is devoted to refractory materials (silicates and carbons) observed in comets. Production and analytical techniques are briefly reviewed, with attention given to the determination of optical properties and the effects of processing. The information derived from experiments aid in identifying major components of comets. Section 3 covers small- and large-scale experiments on the physical properties of ices, while the chemical evolution of ices is described in section 4. The most widely used *in situ* techniques are described, and some of the most relevant recent results are summarized. Some conclusions are given in section 5.

2. EXPERIMENTS ON REFRACTORY MATERIALS

Refractory materials with morphological, chemical, and structural properties suitable to reproduce compounds observed or expected in comets have been produced in the laboratory through various methods of synthesis (e.g., *Colangeli et al.,* 1995; *Rotundi et al.,* 2002; *Nuth et al.,* 2002) and are usually termed cometary dust analogs (hereafter CDAs).

2.1. Production and Characterization Through Spectroscopy of Materials

A wide variety of C- and silicon-based materials are obtained by vapor condensation to form "smokes" (see, e.g., *Colangeli et al.,* 2003, and references therein). In practice, vaporization is achieved by applying sufficient energy to a solid by, e.g., laser bombardment of a homogeneous target or a mixture of different targets (Fig. 1), by arc discharge between C or graphite electrodes (Fig. 1), or by laser pyrolysis in a gas flow. If a metal vapor is present, at its saturation pressure, in a cooling gas-phase mixture, then as the temperature falls molecular clusters can form, which then grow to solid particles. Alternatively, chemical processes, such as sol-gel reactions (*Brinker and Scherer,* 1990; *Jäger et al.,* 2003) or grinding of natural rocks and minerals, can be used to produce a wide variety of CDAs.

A careful selection of experimental conditions during CDA formation allows the "tuning" of the composition and structure of the samples produced. Examples of CDAs produced in the laboratory are summarized in Table 1. It is interesting to note that a wide variety of silicates, in addition to those in Table 1, can be obtained by changing the relative abundance of cations (e.g., Mg^{2+}, Fe^{2+}, Al^{3+}, Ca^{2+}) in the original reaction mixture.

The materials produced in laboratory must be carefully analyzed to check that they are reasonable CDAs and to link their properties to production conditions. A large variety of investigation techniques are based on the interaction of matter with radiation and particles, while other methods are based on the study of mechanical, electrical, magnetic, and thermal properties of matter. All the methods involving interaction of matter with radiation can be classified according to the kind of interaction in microscopy, diffractometry,

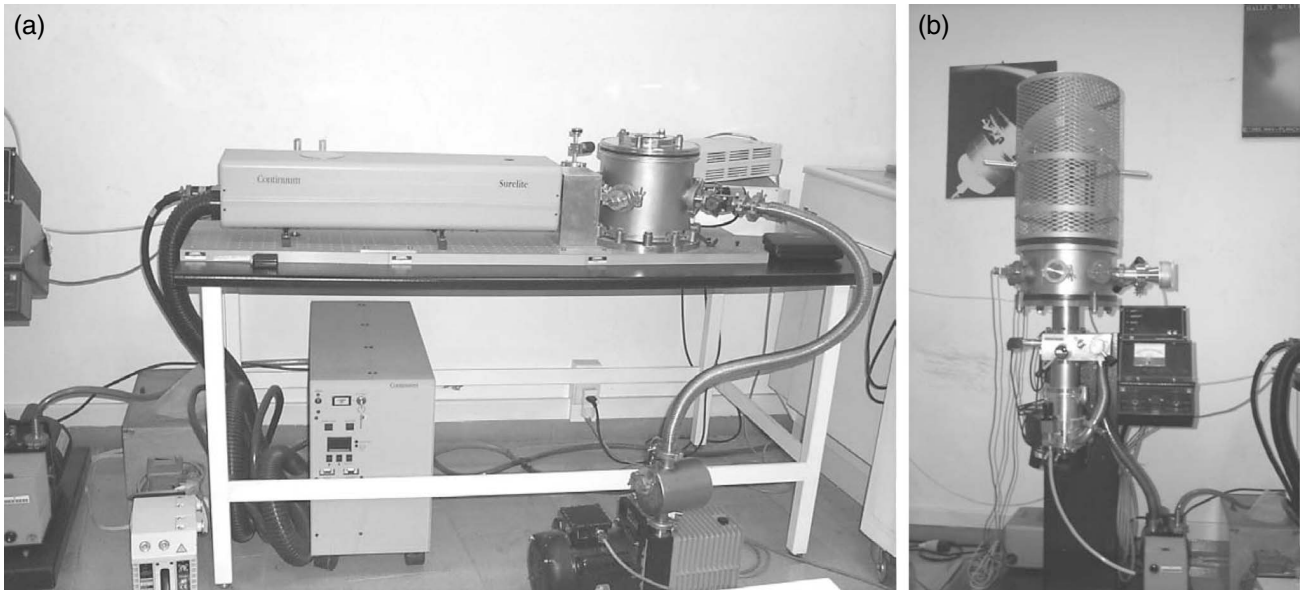

Fig. 1. Methods for condensation of solid grains used at the Cosmic Physics Laboratory of Naples. **(a)** Nd-YAG pulsed laser device for ablation of solid samples in an oxidizing, reducing, or inert atmosphere. **(b)** Device for production of C dust by arc discharge between C or graphite rods in H-rich or inert atmosphere.

TABLE 1. Examples of laboratory cometary dust analogs.

Family	Species	Method of Production
Olivine $(Mg_xFe_{1-x})_2SiO_4$	Forsterite (x = 1)	Laser bombardment in 10 mbar O_2
	Fayalite (x = 0)	Laser bombardment in 10 mbar O_2
Pyroxene $(Mg_xFe_{1-x})SiO_3$	Enstatite (x = 1)	Laser bombardment in 10 mbar O_2
	Ferrosilite (x = 0)	Laser bombardment in 10 mbar O_2
Amorphous C	α-C	Arc discharge in 10 mbar Ar
Hydrogenated amorphous C	HAC	Arc discharge in 10 mbar H_2
		Laser bombardment in 10 mbar H_2
		UV irradiation or ion bombardment of ice mixtures

and spectroscopy. Methods falling in these categories give a vast amount and different kinds of information, unraveling the relations among the properties of solid materials [see *Marfunin* (1995) for a wide and accurate description on methods of investigation on refractory materials]. Many of these techniques are widely used in laboratories to characterize CDAs.

Scanning, transmission, and analytical electron microscopy are used to investigate the morphology and both the short- and long-range structural order of CDAs at nanometer and subnanometer scales (e.g., *Rietmeijer et al.,* 2002; *Fabian et al.,* 2000). These techniques use an electron beam accelerated by high voltage and focused by lenses on the sample surface. The beam is then moved or scanned across the sample area to obtain images providing information on surface structures and morphology (Fig. 2).

Electron and X-ray diffraction are the most frequently used methods to determine the arrangement of atoms in the crystal structure of samples at small and large scales. The analysis is based on the theories of symmetry and on the interaction of radiation with solids. The accuracy of the results of the analysis depends on both sample quality and technique. In particular, X-ray absorption spectroscopy (XAS), extended X-ray absorption fine structure (EXAFS), and X-ray absorption near-edge structure (XANES) techniques are used to determine short- and medium-range order in partially amorphous materials (e.g., *Thompson et al.,* 1996). Elemental composition can be determined by analysis of dispersed X-rays (Fig. 2), while specific aspects of elemental arrangement, such as the ratio of ferrous to ferric iron, can be investigated by wet chemical analyses (*Köster,* 1979).

Raman spectroscopy is another method used to analyze the structure of materials, especially C-based ones. It is based on the process of inelastic scattering of monochromatic radiation hitting the target sample. The Raman scattering consists in the frequency shift of the Raman lines with respect to the exciting radiation and results from the energy exchange between the exciting radiation and the vibrational levels of the materials. Raman scattering is used to identify minerals embedded in matrix in a nondestructive way and is suitable to investigate the structure of minerals by the analysis of the symmetry of vibrational modes. Vibra-

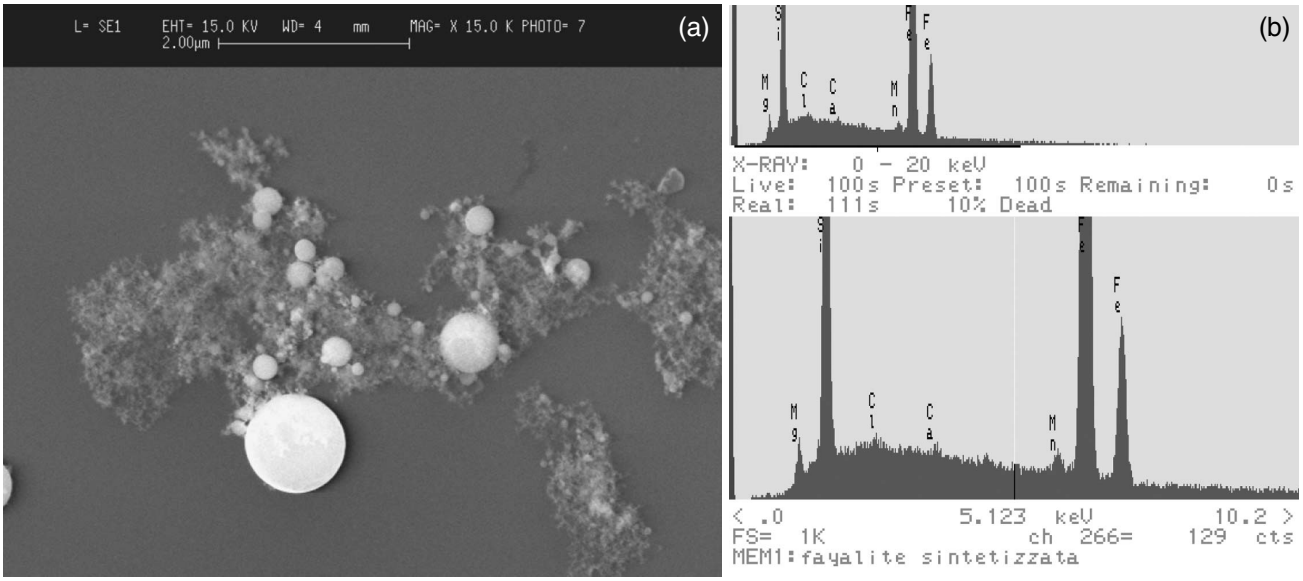

Fig. 2. **(a)** Scanning electron micrograph of amorphous olivine as produced by laser ablation of a pure olivine target. **(b)** Energy dispersive X-ray analysis of amorphous olivine.

tional spectra are highly sensitive to the degree of order of materials. Order/disorder degrees of carbonaceous materials synthesized in the laboratory or present in meteorites and interplanetary dust particles can be investigated with respect to the processing experienced by materials during their life as, e.g., ion irradiation (*Wopenka,* 1988; *Strazzulla and Palumbo,* 2001; *Baratta et al.,* 2004).

Although the techniques described above are fundamental tools for material characterization, spectroscopy remains the most used and powerful way to investigate CDAs. In fact, different aspects of materials can be revealed by different wavelengths of light. Measurements in the vacuum ultraviolet probe electronic transitions of solids, while spectroscopy in the visible region allows the identification of the electronic gap and thus the conduction properties of materials. Midinfrared (IR) light is in the range where molecular vibrational resonances can be excited by incoming radiation, while material structure and morphology drive the spectral behavior in the far-IR region. Therefore, for the study of material characteristics at all scales, a careful investigation over a wide spectral range provides an important complement to information from other analytical techniques. Moreover, results obtained in laboratory by spectroscopic analysis of materials can be used in direct comparison with astronomical observations or by modeling the spectroscopic behavior of dust grains. Details on use of laboratory spectra are described in the following sections.

2.1.1. Extinction and absorption. Considering the extinction and absorption of IR light by dust grains, the dependence of the mass extinction coefficient, $K(\lambda)$, on wavelength, λ, can be derived from measurements on CDAs synthesized in laboratory. The equation

$$K(\lambda) = \frac{S}{M} \ln\left[\frac{1}{T_p(\lambda)}\right]$$

links $K(\lambda)$ to the measured transmittance $T_p(\lambda)$ of a CDA sample of mass M and cross section S, exposed to a radiation beam of wavelength λ. Here $T_p(\lambda) = I(\lambda)/I_0(\lambda)$ is the ratio of the intensities of a light beam after and before meeting a dust sample.

The above relation for $K(\lambda)$ is valid under the assumption that grains interact as separate entities with light, so that multiple scattering is negligible (in other words, the distance between particles is greater than the wavelength of the incident radiation). When the size parameter x satisfies the relation

$$x = \frac{2\pi a}{\lambda} \ll 1$$

with a = grain radius (under the approximation of spherical shape), the scattering contribution to extinction is negligible (see *Bohren and Huffman,* 1983), and $K(\lambda)$ becomes the mass absorption coefficient. Thus the absorption coefficient can be derived directly from transmission IR measurements on submicrometer grains. Three examples of mass absorption efficiency in the IR for silicates and C-based materials are shown in Fig. 3.

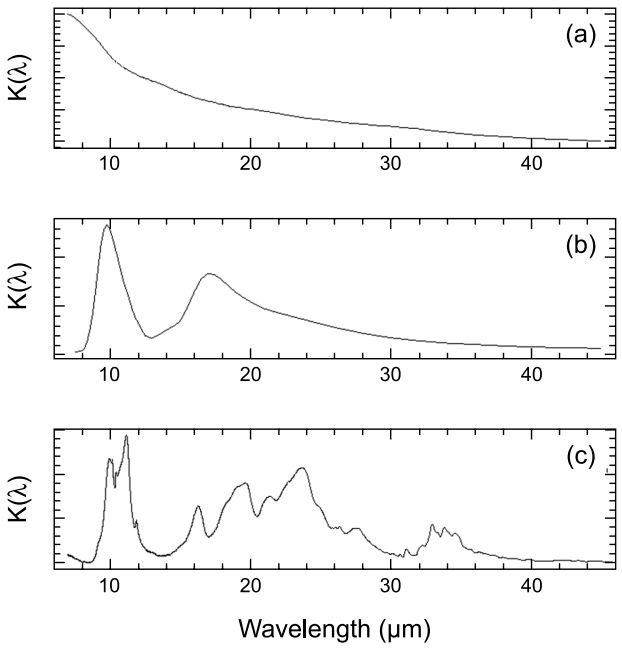

Fig. 3. Mass absorption coefficient (in arbitrary units) of **(a)** amorphous C, **(b)** amorphous olivine, and **(c)** crystalline olivine (*Brucato et al.,* 1999b).

The motivation for determining these mass absorption coefficients is that they can be used to extract information from absorption and emission observations of comets. If scattering is negligible, then the mass column density, β, and the temperature, T, of grains can be obtained under the assumption of equilibrium conditions, for which Kirchhoff's law applies (emittance = absorbance). The cometary emission flux, $F(\lambda)$, is then interpreted as the sum of contributions from N components as

$$F(\lambda) = \sum_{i=1}^{N} \beta_i \cdot K_i \cdot B(\lambda, T_i)$$

where $B(\lambda,T)$ is the Planck function. By fitting $F(\lambda)$ to cometary spectra (see section 2.3), one obtains quantitative information on cometary coma grain properties. This procedure is applicable only if laboratory measurements on $K(\lambda)$ for CDAs are available.

2.1.2. Scattering. Important information on solid materials is provided by an analysis of the light scattering process. Size, shape, and refractive index of particles are intimately correlated to the scattering parameters. Exact theories of light scattering are based on solving Maxwell's equations either analytically or numerically. In the case of spherical homogeneous particles, calculations can be done accurately by using the Mie theory (*Bohren and Huffman,* 1983). Although this simple approximation is used in many applications, real (cometary) dust particles are inhomogeneous and irregular in shape.

To give an accurate description of the phenomenon for irregular particles, the scattering properties have to be either computed theoretically or measured experimentally. Theoretical models, which have become increasingly sophisticated (see, e.g., *Mishchenko et al.,* 2000), use the optical constants of materials and take into account the dependence of the scattering function on morphological properties, such as size and shape. In recent years an effort has been devoted to describe the effects of nonsphericity on scattering properties. In this frame, particles have been classified as solids, aggregates, and clustered particles. *Lumme et al.* (1997) identified particle classes in a mathematical sense as polyhedral solids, stochastically rough (smooth) particles, and stochastic aggregates. Statistical approaches have been used for particles very small compared to the wavelength of radiation (Rayleigh limit), but complications have been encountered in calculations outside the Rayleigh limit. The most important calculation methods can be summarized in two categories: exact theories (separation of variables method for spheroid, finite-element method, finite-difference time domain method, integral-equation methods, discrete dipole approximation, T-matrix approach, superposition method for compounded spheres and spheroids) and approximate theories (Rayleigh, Rayleigh-Gans, anomalous diffraction approximations, geometric optics approximation, perturbation theory). Details on mathematical description of models and their limits and goals are given by *Mishchenko et al.* (2000).

Complementary information that can lead to much improved knowledge of electromagnetic scattering by nonspherical particles is given by laboratory measurements. Randomly oriented ensembles of CDAs with irregular shapes are used in laboratory experiments. The Stokes vectors of the incident and scattered beams are related by a scattering matrix, whose elements are measured vs. the scattering angles (*van de Hulst,* 1957). Usually, measurements in the visible, IR, and microwave spectral ranges are performed. The accurate characterization of CDAs size, shape, and composition, i.e., performed by the analytical techniques described above, allows us to know fundamental parameters that are linked to the scattering parameters (see, e.g., *Hovenier and van der Mee,* 2000; *Muñoz et al.,* 2000; *Volten et al.,* 2001; *Hadamcik et al.,* 2002). A different experimental approach in studying the light-scattering properties of submicrometer grains is to measure microwave scattering by large analog grain samples (*Gustafson,* 1996). In fact, no absolute dimensions are encountered in classical electrodynamics and convenient grain size and electromagnetic wavelength can be chosen. The light-scattering problem can therefore be scaled up or down to any convenient dimension.

The experimental approach can be used to check the quality of results obtained by scattering models. Moreover, measurements are suitable for the direct interpretation of astronomical observations. On this point, we recall that observations of light scattered by particles present in the cometary coma show a linear polarization. The measured phase curves display a negative branch for phase angles lower than 20°, while a positive branch is observed at larger angles with a maximum around 90°–100° (*Levasseur-Regourd et al.,* 1996). Changes in the polarization intensity are observed as a function of the distance from the nucleus, which are attributed to differences in the size distribution and/or color of cometary grains (*Muñoz et al.,* 2000) or to different degrees of grain fluffiness (*Hadamcik et al.,* 2002). The subject is presently matter of further laboratory investigation by using different classes of CDAs (H. Volten, personal communication, 2003).

2.2. Processing of Cometary Dust Analogs

Laboratory CDAs can be energetically processed by different methods to study their evolution and the efficiency of extraterrestrial processes to modify the material's optical, structural, and chemical properties. We consider two examples.

Silicates produced by condensation techniques are subjected to thermal annealing under vacuum, for specific temperatures and times, in order to study variations induced by this process on physical, chemical, and structural properties of the samples. The most striking effects are structural modifications that tend to crystallize amorphous materials (*Hallenbeck et al.,* 1998, 2000; *Brucato et al.,* 1999a, 2002; *Fabian et al.,* 2000). Infrared spectroscopy is an efficient method for monitoring changes caused by thermal annealing. Wide IR absorption bands, typical of amorphous materials, tend to sharpen, as expected for crystalline solids. Such amorphous-to-crystalline transitions can be quantitatively characterized through the activation energy, E_a, defined by

$$t = \nu^{-1}\exp\left(\frac{E_a}{kT}\right)$$

In this equation, t is the time for the material to reach long-range order inside the lattice, ν is a characteristic vibrational frequency of the material, and T is the temperature. Activation energies have been measured in the laboratory for a wide variety of materials that are relevant as CDAs. The results obtained for different silicate species are summarized in Table 2. The implications of these results on the evolution of silicates forming comets will be discussed in the next section.

Both pure-C and H-rich C grains can be produced by the evaporation techniques mentioned in section 2.1. Laboratory experiments on such grains have shown that thermal annealing (*Mennella et al.,* 1995), UV irradiation (*Mennella et al.,* 1996), ion bombardment (*Mennella et al.,* 1997), and interaction with gas (*Mennella et al.,* 1999) are competitive processes that determine chemical and structural transformations.

Among other diagnostic features, infrared C-H stretching modes in the 3.3–3.4-μm range, are suitable both for identifying the amount of H linked to the C structure and for disentangling the most important C structural arrangements. In fact, the IR band intensity is related to the H abundance, with dominant features around 3.3 or 3.4 μm, indicative of

TABLE 2. Activation energies E_a/k (K) for crystallization.

Composition	*Hallenbeck et al.* (1998)	*Brucato et al.* (1999a)	*Fabian et al.* (2000)	*Brucato et al.* (2002)
SiO_2	—	—	49,000	—
$MgSiO_3$	—	47,500	42,040	—
Mg_2SiO_4	45,500	—	39,100	40,400
Fe_2SiO_4	—	—	—	26,300
$MgO\text{-}SiO_2$	—	—	—	45,800
$MgO\text{-}SiO_2\text{-}Fe_2O_3$	—	—	—	<49,700

aromatic (graphitic) vs. aliphatic networks, respectively, forming the grains.

Results of experiments can be summarized as follows: (1) Bombardment of pure amorphous C grains with about 10^{20} H atoms cm^{-2} produces the appearance of a neat aliphatic 3.4-μm band (*Mennella et al.,* 1999). (2) Processing of hydrogenated amorphous C grains by UV irradiation (Lyman emission) or ion bombardment produces a progressive release of H and a transition from an aliphatic-dominated to a more aromatic material (*Mennella et al.,* 1996, 1997). (3) Irradiation of hydrogenated amorphous C grains at fluences of about 10^{19} UV photons cm^{-2} produces a significant decline of the 3.4-μm band, even when the dust is coated by Ar, H_2O, or $H_2O\text{-}CO\text{-}NH_3$ ices (*Mennella et al.,* 2001).

It must be also noticed that UV irradiation and ion bombardment of organic materials produce similar effects, loss of function groups and polymerization (*Jenniskens et al.,* 1993) (see also section 4).

These results provide guidance for following the evolution of C-based materials in different space environments, including comets, as discussed in the next section.

2.3. Interpretation of Cometary Observations by Laboratory Data and Future Steps

The presence of crystalline silicates in comets was first shown by observing the IR spectrum of Comet P/Halley 1986 III. A strong 11.3-μm emission peak was attributed to crystalline olivine grains (*Campins and Ryan,* 1989). A double peak at 9.8 and 11.3 μm indicated that amorphous and crystalline silicates were coexisting components. However, groundbased observations of other comets showed different shapes for the emission features (*Hanner et al.,* 1994). Based on laboratory measurements (e.g., *Colangeli et al.,* 1996), these differences were attributed to the presence of different silicates, whose origins could be traced to different formation conditions and to transformations by various processing mechanisms (Table 3).

The 1997 passage of Comet Hale-Bopp C/1995 O1 provided the first opportunity to observe a new long-period Oort cloud comet, both from the ground and from space. The ISO satellite allowed an examination of cometary grain emission over the full IR range (*Crovisier et al.,* 1997), and led to the discovery of a rich variety of strong distinct emis-

TABLE 3. Mass percentage of submicrometer grains derived from fitting cometary spectra with laboratory absorption data of different materials.

Comet	AU	Crystalline Olivine	Amorphous Olivine	Amorphous Pyroxene	Crystalline Pyroxene	Amorphous Carbon
C/1989 Q1 Okazaki-Levy-Rudenko	0.65*	28	—	—	—	72
C/1989 X1 Austin	0.78*	12	—	—	—	88
1P/1982 U1 Halley	0.79*	33	—	—	52	15
C/1987 P1 Bradfield	0.99*	42	—	—	48	10
C/1983 H1 IRAS-Araki-Alcock	1.0*	—	85	—	—	15
1P/1982 U1 Halley	1.25*	22	—	—	20	58
C/1987 P1 Bradfield	1.45*	24	—	—	23	53
C/1990 K1 Levy	1.51*	20	36	—	—	44
C/1990 K1 Levy	1.56*	19	47	—	—	34
C/1994 E1 Mueller	2.06*	23	—	—	30	48
C/1995 O1 Hale-Bopp	0.97‡	30	17	25	8	20
	1.21‡	23	18	37	4	18
	1.7‡	25	14	33	8	21
	2.8‡	25	25	24	5	21
	2.9†	69	20	—	—	11

**Colangeli et al.* (1996), spectral range 8–13 μm.
†*Brucato et al.* (1999a), spectral range 7–45 μm.
‡*Harker et al.* (2002), spectral range 1.2–45 μm.

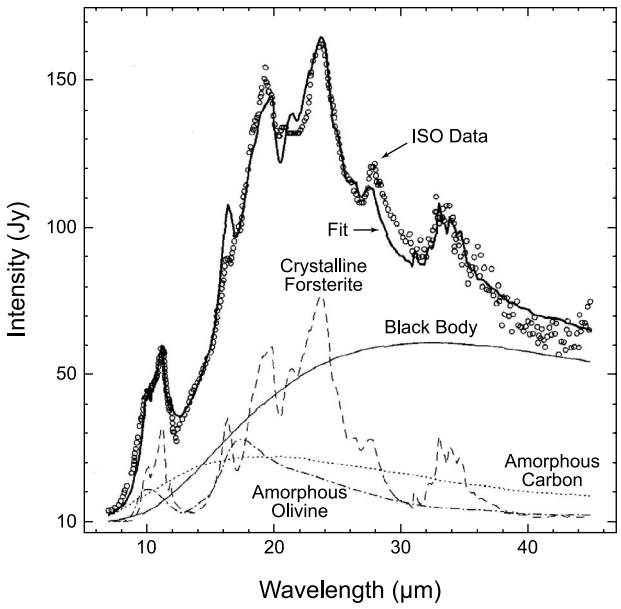

Fig. 4. Fit of ISO observation of Comet Hale-Bopp [circles, *Crovisier et al.* (1997)] with the optical properties of a combination of amorphous and crystalline materials measured in the laboratory (*Brucato et al.,* 1999b).

sion features. Hale-Bopp's IR spectrum was interpreted as due to amorphous and crystalline silicates and amorphous C grains in the coma. A detailed match of all major peaks with laboratory data for silicate grains suggested the identification of crystalline Mg-rich olivine (forsterite) as one of the main components (Fig. 4). Groundbased Hale-Bopp observations at different heliocentric distances (e.g., *Hayward and Hanner,* 1997; *Wooden et al.,* 1999) indicated that a further component of crystalline Mg-rich pyroxene (enstatite) was also present (Table 3).

Different silicate band profiles and peak positions in different comets may be correlated to comet formation and evolution. According to present evolution models, silicates coming from the presolar cloud and infalling onto the protosolar nebula were amorphous. The results obtained from laboratory simulations indicate that amorphous-to-crystalline transformations can only occur on timescales under 10^6 yr if annealing temperatures above ~800 K are reached. It is, therefore, unlikely that amorphous silicates were converted into crystalline materials in the outer nebula, where comets are supposed to have been formed, as the temperature was too low (few tens of Kelvins) to thermally process grains before their incorporation in cometary bodies. A subsequent thermal processing at high temperatures would have been necessary to crystallize them.

Two possible scenarios have been recently proposed to explain the presence of crystalline grains in comets: turbulent radial mixing in the solar nebula (*Bockelée-Morvan et al.,* 2002) and annealing of dust by nebular shocks (*Harker and Desch,* 2002). It has been demonstrated that a flash heating at 1100 K is sufficient to crystallize micrometer-sized particles in few minutes, as has been proposed to happen for precursors of meteoritic chondrules (prechondrules) (*Rietmeijer,* 1998). It has also been suggested that the observed amount of crystalline silicates in cometary grains is an indicator of the age of comets; older comets should be rich in amorphous grains, while younger comets should contain an abundance of crystalline silicates. In fact, it is expected that thermal annealing of amorphous silicate grains present in the hot inner part of the protosolar nebula favors the increase of the fraction of crystalline material over time. Thus, comets formed later in the nebular history will contain a larger amount of annealed (crystalline) dust with respect to those formed earlier. Instead, comets formed very early in the solar nebula should consist almost exclusively of amorphous silicates and unaltered interstellar ices since little processed material was available when they formed (*Nuth et al.,* 2000).

Laboratory studies on olivine grains suggest that the activation energy E_a decreases as the Mg/Fe abundance ratio increases, in contrast with observations that provide no evidence of crystalline Fe-rich silicates. In fact, if both iron and magnesium, with about the same cosmic abundance, were incorporated into silicates forming precometary grains, thermal annealing would favor crystalline Fe-rich over Mg-rich silicates, and their presence should be detectable by IR features. The absence of crystalline Fe-rich silicates could be justified by the presence of iron as pure metal.

As far as C in space is concerned, aromatic and aliphatic C-H IR features are observed in different space environments. Features at 3.38, 3.41, and 3.48 μm have been detected both in the diffuse interstellar (IS) medium (*Pendleton et al.,* 1994) and in the protoplanetary nebula CRL 618 (*Chiar et al.,* 1998). Similar bands are lacking in the dense IS medium, where only a weak 3.47-μm feature is observed, attributed to tertiary C-H bonds (*Allamandola et al.,* 1993). These differences suggest that C suffers modifications in the transition from diffuse to dense clouds. Based on laboratory results (see previous section), the 3.4-μm aliphatic band observed in the interstellar medium and in protoplanetary nebulae is attributed to the prevalence of aliphatic C-H bonds formation by H atom reactions on C grains over the destruction by UV irradiation. In dense clouds, where grains are coated by an ice mantle, the C core is prevented from reaction with H atoms and the C-H bonds are destroyed by penetrating UV photons.

It is interesting to note that a complex of features in the 3.3–3.4-μm range is evident in the emission spectra of comets. Most of these features are due to volatile coma molecules (e.g., methanol, methane, and ethane). Excess emission, once the molecular contribution is accounted for, is attributed to a solid C component (*Davies et al.,* 1993).

The applications reported above clearly evidence the relevance of laboratory experiments on refractory materials in the identification of cometary species. Despite the fact that important results have already been obtained, many open points remain to be clarified and require further ex-

perimental work. The genesis of the crystalline component, specifically concerning the cometary silicates, is still a matter of debate. Besides the interpretation reported above about turbulent radial mixing and flash heating by shock, the possibility exists that amorphous silicate grains lie in an energetic metastable state, produced, e.g., by ion irradiation. In this case, little energy would be required to allow the amorphous-to-crystalline transition. Of course, the validation of this scenario needs support from dedicated laboratory experiments. As far as carbons are concerned, the relations between the solid and the molecular phases in comets are still not well understood. Future experiments shall have to be oriented to clarify the chemistry related to energetic processes, such as UV irradiation and ion bombardment, under conditions that are representative of comet environment, at different stages of their evolution.

3. EXPERIMENTS ON THE PHYSICAL STRUCTURE OF COMETARY ICES

Observations of cometary comae can reveal, although not completely, the composition of cometary ice, namely the gases trapped in the water ice in the nucleus and their proportions relative to water. In turn this information can tell us about the gas composition and temperature in the region where ice grains formed, grains that later agglomerated to form comet nuclei. Ice grain formation may have occurred in the cold and dense IS cloud, which collapsed to form the solar nebula or by water condensation on grains at the cold outskirts of the solar nebula itself. In both scenarios, water vapor adhered to mineral grains and formed H_2O-ice in the presence of gases, which could be then trapped in the ice itself. These trapped gases are released from the ice during changes in its structure and *not* according to their sublimation temperatures. This is evident from the simultaneous release of all the gases observed in the coma of Comet Hale-Bopp over many heliocentric distances by *Biver et al.* (1999).

3.1. Small-Scale Studies

When vapor-phase H_2O molecules condense into ice below ~120 K, they lack the energy to migrate and form a stable crystalline structure. Rather, they remain where they strike, forming an amorphous ice structure with many open pores. Any other gas molecules present can then enter these pores, adhere to the walls through Van der Waals forces, and remain in the pores for a certain time. If additional H_2O molecules arrive by then and condense, the pores can be closed, trapping the gas inside the ice. Some molecules are more readily trapped than others, which can lead to selective trapping of the molecules from the gas-phase mixture, with important implications. For example, it has been shown experimentally that among the heavy noble gases, the trapping preference is Kr > Xe > Ar (*Owen et al.,* 1991, 1992) due to (1) the different polarizabilities of these atoms and therefore different adherence to the walls of the ice pores, (2) differences in their masses (*Notesco et al.,* 2003), and (3) their sizes. This Ar/Kr/Xe pattern in cold H_2O-ice agrees well with the noble gas ratio in Earth's atmosphere, suggesting that comets may have delivered most of these gases to the forming Earth (*Melosh and Vickery,* 1989; *Chyba,* 1987, 1990; *Pepin,* 1997; *Owen and Bar-Nun,* 1993, 1995; *Notesco et al.,* 2003), along with other cometary volatiles such as CO, CO_2, CH_4, N_2, NH_3, HCN, and H_2S.

Moreover and most important, the high HDO/H_2O ratio in Earth's oceans, which could not have been obtained if the water was in chemical equilibrium with the H_2 and HD in the solar nebula, suggests that comets rich in HDO/H_2O delivered a considerable fraction of Earth's water and volatiles (*Laufer et al.,* 1999). The high HDO/H_2O and DCN/HCN ratios in Comets Halley, Hyakutake, and Hale-Bopp (*Eberhardt et al.,* 1995; *Despois,* 1997; *Bockelée-Morvan et al.,* 1998; *Meier et al.,* 1998) suggest that their water originated in the ISM, where ion-molecule reactions enriched the amount of HDO over H_2O, and also suggest that this water never equilibrated with the HD and H_2 in the solar nebula. A cold origin for ice grains is also inferred from the ~22–27 K required for the trapping of CO in ice, needed to account both for the ~7% of CO/H_2O in the comae of Comets Halley, Hyakutake, and Hale-Bopp (*Irvine et al.,* 2000) and the 25 K derived from the ortho-para spin ratio of H_2O in Comets Halley (*Mumma et al.,* 1988) and Hale-Bopp (*Crovisier,* 1999) and the ortho-para ratio of NH_3 in Comet LINEAR (*Kawakita et al.,* 2001). It seems therefore that the ice grains that agglomerated to form these and other comets originated in very cold regions either in the collapsing dense interstellar cloud or in the very cold outskirts of the solar nebula.

Many experiments (e.g., *Bar-Nun et al.,* 1985, 1987; *Laufer et al.,* 1987; *Schmitt and Klinger,* 1987; *Sandford and Allamandola,* 1988; *Schmitt et al.,* 1989a,b; *Hudson and Donn,* 1991; *Jenniskens et al.,* 1995; *Notesco and Bar-Nun,* 1997) have shown that gases in the presence of condensing water vapor can be trapped and distributed within the frozen H_2O, and that they do not simply freeze out as segregated molecules. More detailed studies were carried out by *Jenniskens and Blake* (1994) and *Jenniskens et al.* (1995) on the structure of amorphous ice around 22–30 K.

Another mechanism by which gases can be trapped is the formation of clathrate hydrates, in which H_2O molecules form cages around guest atoms or molecules. However, experiments have shown that while polar molecules, such as CH_3OH, H_2S, C_4H_8O (tetrahydrofurane), and C_2H_4O (oxirene), can form clathrate hydrates (*Blake et al.,* 1991; *Richardson et al.,* 1985; *Bertie and Devlin,* 1983), some of the most prominent cometary gases, such as CO, CO_2, CH_4, and NH_3, do not. The latter molecules are not trapped as clathrate hydrates even in the presence of a clathrate-hydrate-forming gas such as CH_3OH (*Notesco and Bar-Nun,* 1997, 2000).

When the H_2O-ice is warmed, how do the trapped gases escape? Near 120 K (*Schmitt et al.,* 1989a) H_2O molecules in the amorphous ice acquire enough energy to move and rearrange into the more-stable cubic structure, although about 70% of the ice remains in a "restrained amorphous" form,

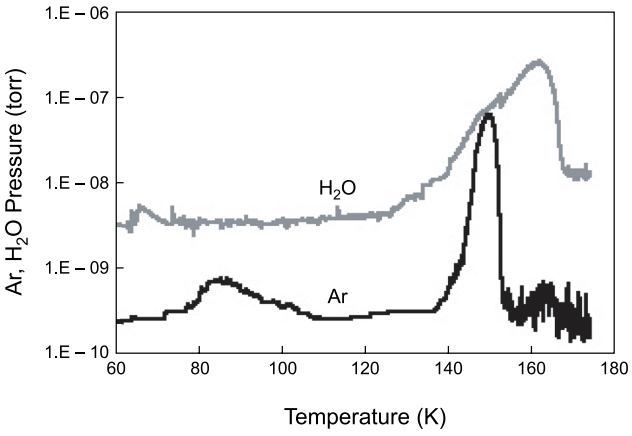

Fig. 5. Gas evolution from a 0.1-μm amorphous gas-laden ice sample upon its warming up. The gas comes out when the amorphous ice transforms into its crystalline and "restrained amorphous" forms.

which is a viscous liquid at this temperature (*Jenniskens and Blake,* 1994, 1996; *Jenniskens et al.,* 1995, 1997). This movement opens pores in which the trapped gases reside, and releases them (Fig. 5). Therefore, all the trapped gases come out together and not according to their sublimation temperatures (*Biver et al.,* 1999).

When heat is applied to a collection of gas-laden ice grains, two gas-release steps occur (Fig. 5). First, near ~120 K, each grain releases the gas trapped within by a dynamic percolation process, in which channels in the ice open up to the surface of the grain (*Laufer et al.,* 1987). Next, a gas molecule leaving an individual grain must still pass near other ice grains in order to emerge from the bulk of the ice. This involves another dynamic percolation process, in which channels open between the grains up to the surface. The ejection of ice grains when a large flux of gas emanated from the ice was observed experimentally by *Laufer et al.* (1987). These processes were modeled (e.g., *Prialnik and Bar-Nun,* 1992), using available experimental data on thin (0.01–100-μm) ice samples. Yet, in order to study large-scale phenomena, large ice samples have to be studied.

3.2. Large-Scale Studies

The first large-scale cometary ice experiment was the Comet Simulation (KOSI) series of experiments carried out at the German Aeronautic and Space Organization (DLR) in Köln. A space simulator of 2.5-m diameter and 4.9-m length, capable of reaching 10^{-6} Torr and having an assembly of Xe-arc lamps capable of illuminating a 30-cm-diameter sample with 1–1.4 solar constants was used (*Grün et al.,* 1991). The comet analog, 30 cm in diameter and 15 cm thick, was produced by spraying fine droplets of a slurry of minerals in liquid H_2O into liquid N. Such ice was always crystalline and *not* amorphous and so could not trap gases in it, as does amorphous cometary ice. In order to add gas to the solid mixture, CO_2 was flowed into the mineral-crystalline ice mixture in liquid N and froze there. The canister at 80 K, containing a mixture of ~10% minerals with traces of C soot, crystalline ice, and 0–15% frozen CO_2, all in liquid N, was placed in the vacuum chamber, where the liquid N evaporated, leaving behind a porous sample with a density of ~0.5 g cm^{-3}. When the powerful "sun" was turned on, a vigorous response from the 45° inclined sample was observed, in which water vapor from the surface and frozen CO_2 from both the surface and from deeper layers sublimated as the heat wave penetrated inward. Driven by these gases, mineral grains were ejected. After a while, a mineral dust layer free of ice accumulated on the surface, slowing down the activity, apparently due to its poor thermal conductivity. These observations were accompanied by measurements of several types:

1. Heat was transported through the sample, illuminated by 1–1.4 solar constants, with dark periods. A representative data plot is shown in Fig. 6a. As expected, ice layers closer to the surface heat faster and the inner layers lag behind. The same trend was observed when the heating was

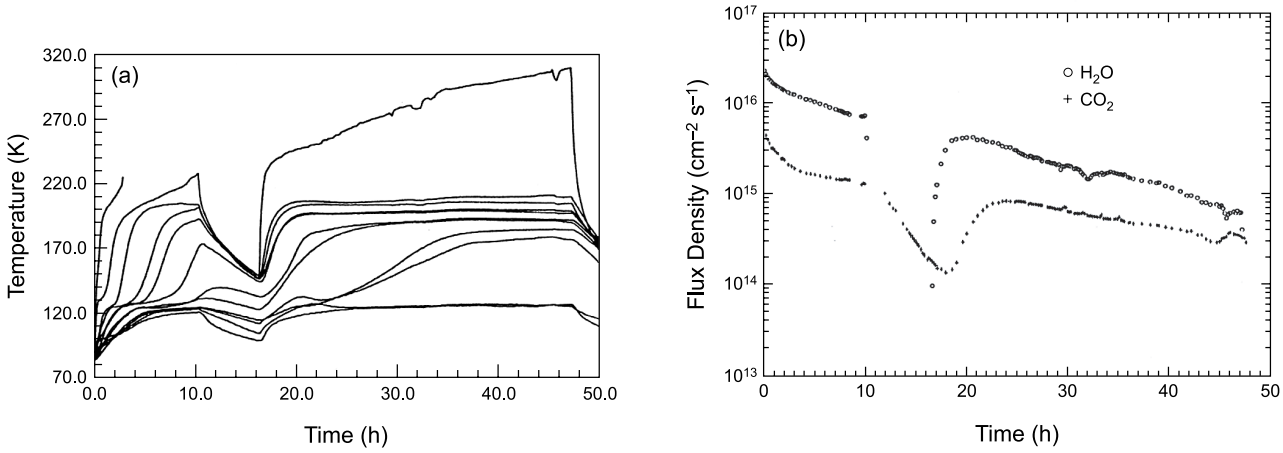

Fig. 6. **(a)** Evolution of temperatures in KOSI-3 sample at different distances from the cold backplate. **(b)** H_2O and CO_2 gas flux densities at the sample surface (KOSI-3).

stopped and resumed. The thermal conductivity of various KOSI samples was calculated from such measurements and found to be about $1–6 \times 10^4$ erg cm^{-1} K^{-1} s^{-1}, depending on the ratios of minerals/hexagonal ice/frozen CO_2. These values are about an order of magnitude smaller than the value for a block of hexagonal ice, $3.5–8 \times 10^5$ erg cm^{-2} K^{-1} s^{-1} (*Spohn et al.,* 1989), due to the porosity of the KOSI samples.

2. Gas emission was studied by the mass spectrometers (Fig. 6b) (*Grün et al.,* 1991). Immediately when insolation began, a flux of $H_2O/CO_2 \approx 6$ (the ratio in the original sample was 5.6) was measured, decreasing to ~3 after 50 h of illumination. When the insolation was interrupted, the H_2O flux dropped immediately, whereas the CO_2 flux lagged, decreasing over 18 h. When the insolation was resumed, the H_2O flux rose during about 2 h, whereas the CO_2 took about 5 h to rise. This is reasonable, because although the water vapor came from the surface at the beginning and from just below the dust mantle, the frozen CO_2 sublimated from deeper layers that took longer to warm up. Generally, the flux of both gases diminished by 2 orders of magnitude (from H_2O 10^{18} to 10^{16} cm^{-2} s^{-1}) after 50 h, due to the formation of an insulating dust layer and the depletion of both volatiles from the upper layers of the ice.

3. During the sublimation of water and CO_2, a very large flux of mineral and ice-coated mineral grains was ejected. The ejected material was photographed with a video camera, grain impacts were monitored by microphones facing the sample, and particles were collected over a large sampling area. The erratic flux of grains diminished by about 2 orders of magnitude during 10 h, along with the diminishing flux of gas and water vapor. A median velocity of ~100 m s^{-1} was obtained. This result is not far from the value (≥167 m s^{-1}) observed experimentally by *Laufer et al.* (1987) for ice grains ejected from a thin ice sample, when a large flux of gas was released.

In another experiment (*Mauersberger et al.,* 1991), individual particles entered a tube with a pressure gauge, where they were heated and their volatiles sublimated. Two types of traces were measured: sharp spikes decaying within a few seconds, apparently from pure ice grains, and much broader ones, decaying over tens of seconds, apparently from ice-containing porous mineral particles. The structure of the collected grains was studied by SEM and found to be very fluffy (Fig. 7), with a density of about 0.1–1 g cm^{-3}. They seemed to be an agglomerate of even smaller grains, not unlike the interplanetary dust particles (IDPs) collected in the stratosphere (*Brownlee et al.,* 1980). These agglomerates of mineral particles were formed in the slurry of water and minerals that was sprayed into the liquid N, but it is possible that some could have formed in the ice during its sublimation. Occasionally, a dust grain still attached at one point to the mantle would vibrate violently for many minutes, driven by the gas flux, until finally it flew away. Some dust bursts were observed when a larger chunk of material fell back onto the surface.

After many hours of insolation, the chamber was opened and the sample container was transferred to a bath of liquid N in a N purged glove-box. Its compressive strength was measured by driving a force meter into the sample. The initial strength of $1–2 \times 10^6$ dynes cm^{-2} was increased after insolation to $0.4–5 \times 10^7$ dynes cm^{-2} just below the dust mantle, probably due to the migration of some water vapor inward, and its freezing there. Reflectance spectra of the surface between 500 and 2500 nm were measured and, as expected, showed that the CO_2 and H_2O features diminished considerably.

Similar large-scale experiments were carried out by *Green et al.* (1999) and *Green and Bruesch* (2000) at the Jet Propulsion Laboratory (JPL) in Pasadena, California. A slurry of minerals in water was sprayed into liquid N, again producing hexagonal ice, in a 200-cm-wide and 250-cm-high cylindrical canister, with an insolation of 0.1–2.1 solar constants. The penetration of the heat wave was monitored by thermocouples; the evolution of water vapor was measured by two mass spectrometers, and dust release by a video camera. The mechanical properties were measured in the closed chamber by a mechanical penetrator-scratcher and, when the chamber was opened, measurements on compressive strength, penetrability, porosity, and density were car-

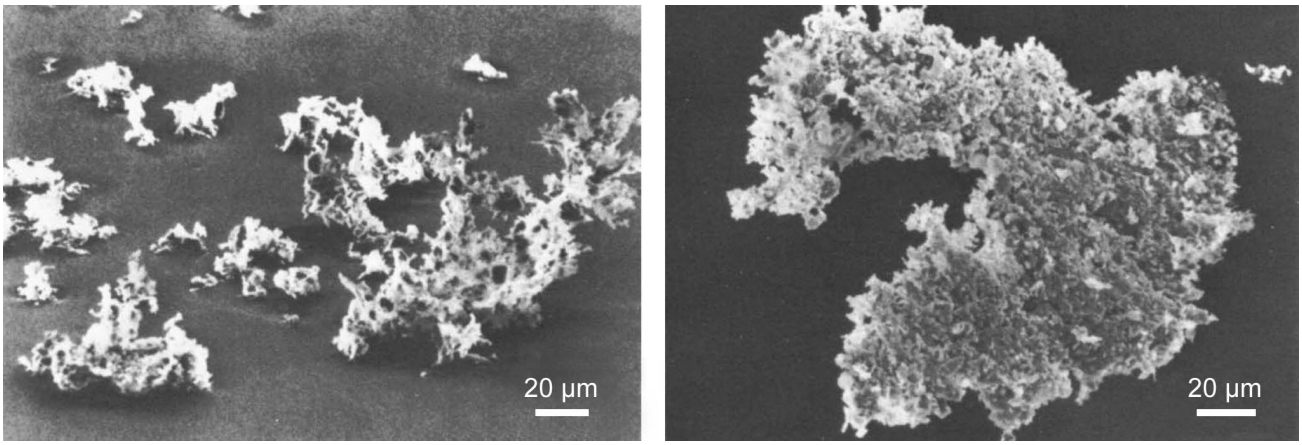

Fig. 7. SEM micrographs of dust grains emitted during the KOSI-3 experiment.

ried out. The results of these measurements are not yet available in the literature.

Although the extensive and detailed KOSI and JPL projects opened a new field of large-scale comet simulation, they suffered from a basic drawback due to the method of sample preparation, namely spraying a slurry of ~10% dust in water into liquid N. This resulted in crystalline ice, which could not trap gases. The added CO_2 (up to CO_2/H_2O ~0.2 in the KOSI experiment) was frozen among the H_2O-ice particles and not actually trapped in amorphous H_2O grains, which is the most relevant situation inferred from comet observations (co-evolution of all gases and water vapor together) and from the extensive small-scale laboratory studies. These small-scale experiments have shown that trapping of ~10% CO in cometary H_2O-ice grains at a very slow deposition rate requires temperatures of ~22–27 K, where the ice formed by vapor deposition is amorphous and full of pores. Yet amorphous ice can be produced even at 80 K, with some structural differences from ice formed at ~30 K, but still well below the ~120-K transformation temperature and gases can be trapped in it.

3.3. Studies of Large Samples: Gas-Laden Amorphous Ice Samples

The next step in large-scale comet simulation was to produce a 200-cm^2 × 10-cm-high sample *of* amorphous ice, with gases trapped inside, although with no mineral dust (*Bar-Nun and Laufer,* 2003). The main objective of this study was to learn how much gas is released to the sample's surface during the crystallization of the ice in deeper layers vs. the flux of water vapor released by sublimation on the surface. The relevant cometary issue is the gas/water vapor ratio in the coma vs. its ratio in the nucleus. Other ice properties, such as heat conductivity, which is of prime importance to models, and compressive strength, which is important for comet splitting and for landing on the nucleus, were also measured in this work.

Large samples of amorphous ice cannot be produced by depositing H_2O vapor onto a cold plate, as is routinely done in small-scale experiments. With large samples the problem of removing the water's heat of condensation (2.7×10^{10} erg g^{-1}) is more severe, especially as amorphous ice has a low thermal conductivity (<~10^4 erg cm^{-1} K^{-1}). If one grows too thick an ice layer, the heat of condensation cannot be removed by the underlying cold surface, so that the newly deposited layers reach ~120 K and become crystalline rather than amorphous. Consequently, even if a gas flow accompanies ice formation, no gas trapping occurs. To solve these problems, thin ~200-μm ice layers were formed at 80 K (liquid N) on a cold plate, through which the heat of condensation could still be transmitted to the cold surface, remain amorphous, and trap the accompanying gas. Once a thin amorphous gas-laden ice layer formed, it was scraped from the cold plate by a 80-K cold knife into the 80-K sample container, which was covered by an 80-K dome. All these parts, as well as the heat shield surrounding the entire chamber, were kept at 80 K by a controlled flow of liquid N. This fully automatic, hydraulically controlled process was repeated at 10^{-5} torr for 10–20 h until a large enough ice sample accumulated, namely a 200-cm^2 × 10-cm-high sample of an agglomerate of 200-μm particles of amorphous gas-laden ice. The sample was then covered by the 80-K deposition plate while the dome was heated to ~330 K. When the plate was removed, the sample was illuminated from above by the heated irradiation dome, made of a roughly surfaced aluminum that behaves like a black body at 330 K, with a flux of 5×10^5 erg cm^{-2} s^{-1} at better than 3% uniformity. Since water is practically opaque to IR at the 330-K blackbody spectrum, the energy input of the irradiation dome was totally absorbed by the upper layers of the ice sample.

Ten thermocouples (types E and T) were embedded in the ice, recording the temperature profile of the sample. A mass spectrometer recorded the emission of gas and H_2O vapor during heating, through a 2-cm hole in the dome right above the center of the sample. The sensitivities to various gases provided by the manufacturer were checked by analyzing mixtures of gases with known compositions. The ice density was measured by collecting a small sample in a 1-cm^2 × 5-cm glass vial simultaneously with the large ice sample, and measuring its volume at 80 K and again when melted. The compressive strength was measured by inserting a force-meter penetrator, cooled to 80 K, into the ice, immediately after the experiment was terminated and the chamber was opened. A schematic drawing of the machine is presented in Fig. 8.

To test whether indeed a sample of amorphous ice was produced, Ar was flowed onto the 80-K cold plate by itself and, in a separate experiment, accompanied by H_2O vapor. As expected, Ar by itself did not freeze on the 80-K cold plate, but when accompanied by H_2O vapor, it was trapped in the amorphous H_2O-ice that formed. As learned from studies of thin ice samples, CO behaves like Ar (*Bar-Nun et al.,* 1987). In several experiments, 200-cm^2 × 0.5-cm thick and 200-cm^2 × 6-cm-thick ice samples were produced. The density of the loose agglomerate of 200-μm ice grains was found to be 0.25 g cm^{-3}. This should be compared with the densities of 0.3–0.7 and 0.29–0.83 g cm^{-3} calculated for Comets Halley (*Rickman,* 1989) and Borrelly (*Farnham and Cochran,* 2002), respectively, which contain also mineral particles.

During the ice's heating, the fluxes of sublimating water vapor and Ar were monitored by a mass spectrometer until all the ice sample sublimated. The mass spectrometer record of H_2O and Ar during the entire experiment is shown in Fig. 9a.

Several interesting results came out of this experiment: (1) As stated above, Ar was trapped in the 80-K ice, whereas by itself it was not frozen on the cold plate. This showed definitely that the ice made by this method was amorphous, since only amorphous ice traps Ar in it, while being formed. (2) The time-integrated mass spectrometer fluxes gave Ar/H_2O = 1.01, in comparison with the 1 : 1 ratio in the flowed

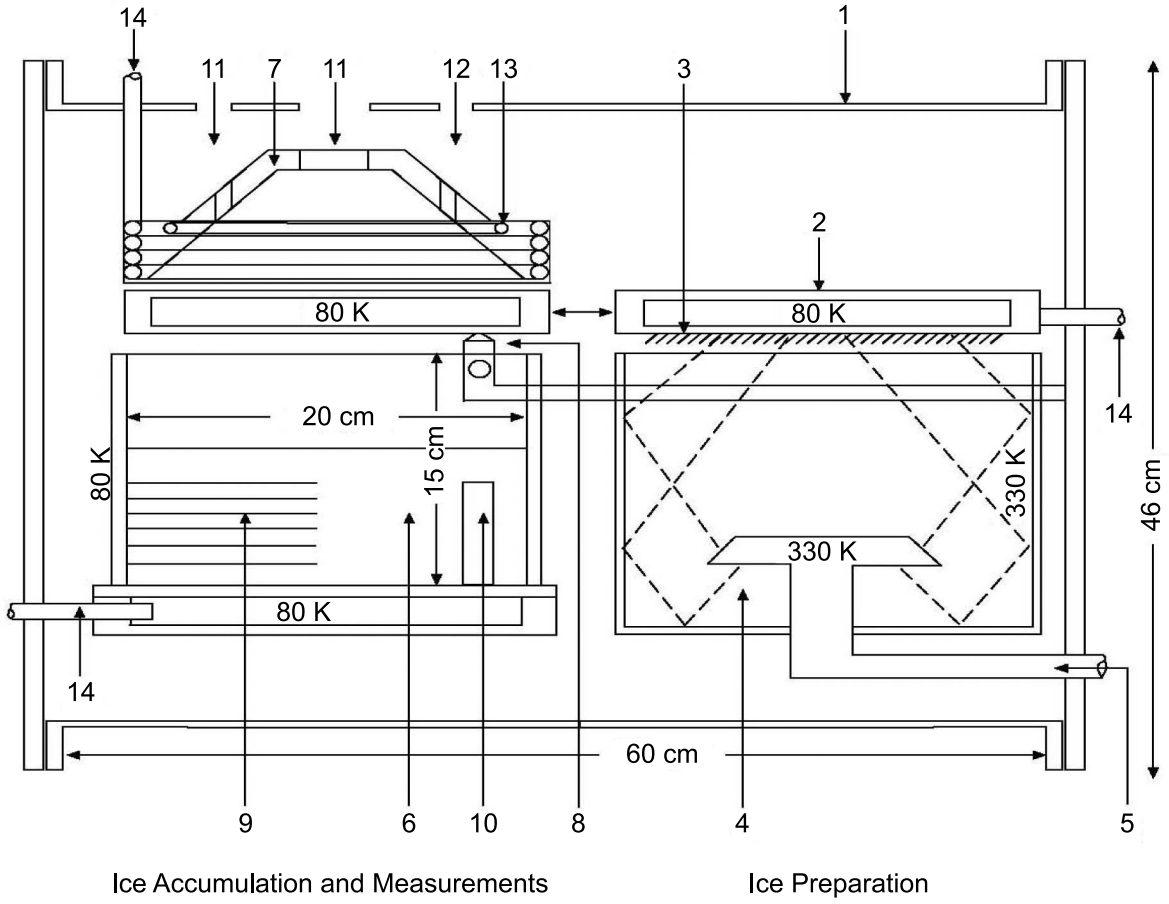

Fig. 8. A schematic drawing of the machine producing large (200 cm^2 × 10 cm) gas-laden amorphous ice samples, as a "comet" simulation: 1 = vacuum chamber, 2 = cold plate at 80 K, 3 = 200-μm amorphous gas-laden ice, 4 = homogeneous flow of water vapor and gas, 5 = water vapor and gas pipes, 6 = 200-cm^2 and 5–10-cm-thick ice sample, 7 = heating dome, 8 = 80-K cold knife, 9 = thermocouples, 10 = density measurements, 11 = mass spectrometer, 12 = ionization gauge, 13 = heating tape, 14 = LN_2 cooling pipes.

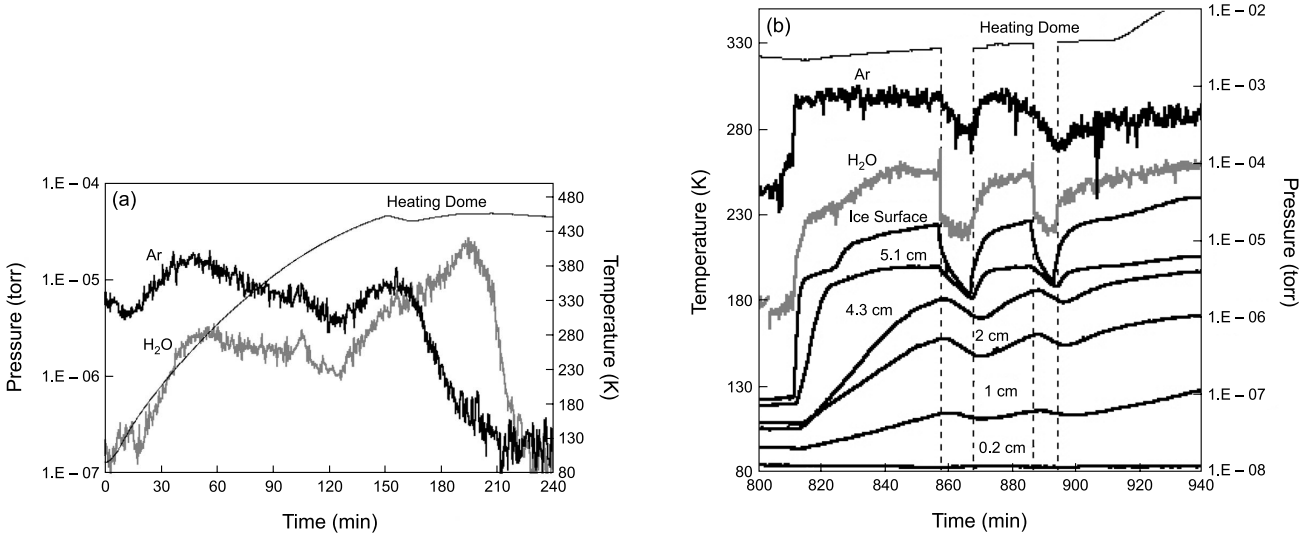

Fig. 9. **(a)** Evolution of Ar trapped in the ice and ice sublimation, upon heating from above of a 0.5-cm-thick sample. Note the early rise of the Ar and its exhaustion before all the ice sublimates. **(b)** Temperature profiles of the thermocouples as a function of their distance from the 80-K bottom plate in a 6-cm-thick ice deposit. Note also the sharp decrease and increase of the water flux vs. the sluggish response of the Ar emanation, when the ice sample is covered by the cold plate and upon its removal.

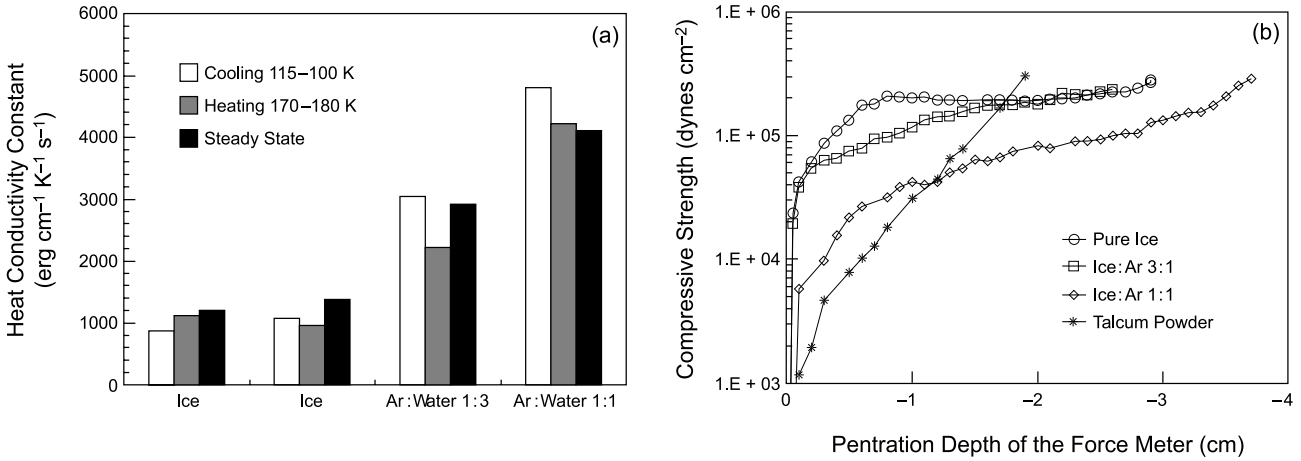

Fig. 10. **(a)** Heat conductivity constant of various ice samples measured at different temperature ranges. **(b)** Compressive strength of the studied ice samples as function of the penetration depth in the ice.

mixture. This result implies that all the Ar was trapped in the amorphous ice and was released upon warming up of the entire 0.5-cm-thick ice layer. (3) The timing and magnitude of Ar evolution from the ice, as seen in Fig. 9a, is of prime importance for the interpretation of comet observations. Even in a 0.5-cm-thick ice layer heated from above, the Ar flux rose to a level about seven times higher than that of the water vapor. This was because the Ar was released from the amorphous ice during the transformation into the cubic and "restrained amorphous" forms, as was found in numerous studies of thin ice samples. This process occurs in the interior of the sample, supplying gas to the experimental "coma," whereas the water vapor emanates only from the ice surface. Eventually, the heated ice layer is exhausted of its gas, as can be seen in Fig. 9a. The Ar flux declines well before all the H_2O-ice sublimates. This raises the question of what the gas/H_2O ratios in cometary comae tell us about gas abundance ratios in cometary nuclei.

Figure 9b shows the thermal history of a 6-cm-thick ice sample, measured through five thermocouples, and the mass spectrometer records of water and Ar release. At 812 min (after the beginning of ice formation) the sample was exposed to the 330-K heating dome. As expected, the ice temperature rose very steeply on the surface and more sluggishly below it. This allowed the thermal conductivity of the ice to be determined. When the heating dome was blocked at 858 min, the surface temperature dropped immediately, whereas the temperature of the deeper layers lagged. The thermal conductivity of the 0.25 g cm^{-3} agglomerate of 200-μm grains of amorphous ice can be calculated from the temperature profiles of the thermocouples embedded in the ice sample, and is shown in Fig. 10a. The heat conduction coefficients of amorphous and cubic water ice were calculated by *Klinger* (1980) to be 2–3 × 10^4 and 2.8 × 10^5 erg cm^{-1} K^{-1} s^{-1} respectively. In the KOSI experiments, on hexagonal porous crystalline ice, the heat conduction coefficient derived was 3–6 × 10^4 erg cm^{-1} K^{-1} s^{-1} (*Spohn et al.,* 1989; *Benkhoff and Spohn,* 1991; *Seiferlin et al.,* 1996).

From recent experiments (Fig. 10a) the heat conduction of gas-free ice is 30 times smaller than Klinger's value for a block of amorphous material [a very much lower thermal conductivity value by a factor of 10^{-4}–10^{-5} was reported by *Kouchi et al*. (1992), but was not measured in other experiments]. This lower value is due to the fact that the sample is an agglomerate of ~200-μm ice particles, and the heat conduction between the grains is poor. One cannot exclude the contribution of inward-flowing water vapor to the thermal conductivity, but it should be noted that no harder crust was detected below the surface, as would have been expected if a massive flow of water vapor froze in deeper layers. Nevertheless, the thermal conductivity of gas-laden ice is much higher than that of pure H_2O-ice, and even more so when the gas content is even greater ($Ar : H_2O$ = 1 : 3 vs. 1 : 1). This shows the importance of trapped gas for the conduction of heat into the interior of comets.

At this stage it is not possible to measure the effect of the exothermicity of the transformation amorphous to cubic ice on the temperature profile. Possibly, this process may be even somewhat endothermic in the presence of trapped gases (*Kouchi and Sirono,* 2001).

The measurement of mechanical properties is rather simple. Pressing a force-meter cooled to 80 K into the extremely fluffy ice produced the results shown in Fig. 10b. As the ice was compressed, its compressive strength increased as its open spaces decreased. Pure ice is "stronger" whereas the Ar trapped in the ice "weakens" it, since the ice particles that form the sample are fluffier. The compressive strength does, however, reach a finite limiting value. During heating, when the Ar left the ice, the fine ice structure collapsed. A very low compressive strength of ~2 × 10^5 dynes cm^{-2} can be deduced from the experiments. For comparison, in the KOSI experiments, in which mineral

grains were mixed with hexagonal ice grains or were covered by a layer of hexagonal ice, the compressive strength was 3×10^5–2×10^7 dynes cm^{-2}, depending on the mineral content (*Jessberger and Kotthaus,* 1989).

3.4. Summary and Implications of Large- and Small-Scale Studies

By studying Ar : H_2O (1 : 1) at 80 K in the large chamber, it was proven that the ice is amorphous, since Ar does not freeze at 80 K but was trapped in the amorphous ice. Large samples of 200 cm^2 × 6 cm, of an agglomerate of 200-μm ice particles of this amorphous gas-laden ice were produced and studied for the first time. These samples can represent pristine cometary nuclei and their still-unprocessed interiors. Yet we should remember that the ice samples did not contain mineral and organic dust and, consequently, the buildup of an insulating dust layer and its subsequent effect on the penetration of the heat wave could not be studied.

The most important finding was that the ratio of Ar/water vapor in the experimental "coma" was between 7 and 10 (Fig. 9) times larger than the Ar/ice ratio in the experimental "nucleus". In the 0.5-cm-thick samples, the Ar was exhausted from the ice well before the ice sublimated completely but in the 6-cm-thick sample, Ar kept emanating from deeper layers (Fig. 9b). This observation has direct bearing on the correlation between the gas/water vapor observed in cometary coma and the gas/ice ratio in the nucleus: The ~10% of CO to water vapor seen in the comae of Comets Halley, Hyakutake, and Hale-Bopp might well mean that the CO/ice in these nuclei could be closer to 1%.

In Comet Hale-Bopp (*Biver et al.*, 1999), the CO flux at 5.2 AU preperihelion was ~6 times larger than the water flux, but became ~5 times smaller than water at perihelion. Apparently, the upper layers were exhausted and gases came out only, and more slowly, from deeper layers. A model incorporating all new results is now being prepared.

Finally, the low density and compressive strength, which attest to the fluffy structure of the ice, can account for breakups of cometary nuclei and should be of concern for the *Rosetta* lander (*Hilchenbach et al.,* 2000). However, incorporating about ~25% mineral dust and about 25% of organic "CHON" particles, as found for Comet Halley, may harden the surface somewhat.

As for small-scale ice studies, much more has to be learned about the preferential trapping of CO over N_2, since no N_2^+ was observed by *Cochran et al.* (2000, 2002) in various recent comets where CO was observed. The enrichment in Earth's atmosphere of the heavier Xe isotopes is still an open problem, although the Ar and Kr isotopic enrichments, when trapped in ice according to their inverse square root of the mass, account for their relative abundances (*Notesco et al.,* 2003). A major problem remains as to how Jupiter obtained its abundances of C, N, O (?), S, P, etc., relative to H_2, as these abundances are ~3 times the solar abundances. It is possible that late bombardment by comets devoid of H_2 could have contributed these volatiles.

4. EXPERIMENTS ON CHEMICAL REACTIONS IN COMETARY ICES

The previous *Comets* book (*Wilkening,* 1982) listed 35 chemical species observed in cometary spectra, but a mere three stable molecules (CO, HCN, CH_3CN). Since then, the cometary molecular list has grown to include about 20 reasonably stable members. As comets are considered to be the solar system's most primitive bodies, it is reasonable to ask how they came to acquire molecules as complex as ethane, methanol, and formamide. Laboratory investigations can help with this question by revealing chemical reactions and conditions that lead to observed cometary species.

It is generally accepted that at each stage of a comet's history, cosmic rays and energetic photons (UV or X-rays) can drive chemistry in cometary ices. Although uncertainties remain in determining precise energy inputs, Table 4 shows values thought to be typical. We note that the chemistry initiated by ionizing radiations, such as 1-MeV protons or X-rays, results mostly from the secondary electrons generated. This means that the observed products, and their abundances, are more dependent on the energy input than the initial carrier of the energy. Since doses on the order of 1 eV per molecule (Table 4) are attainable in the laboratory, experiments to mimic cometary ice chemistry can be performed. In most cases, the differences in photochemical and radiation chemical effects are typically not in the nature of the products made, but rather in product abundances or the depths at which products form in ice samples.

Goals motivating laboratory work on cometary chemistry include the following: (1) Discovery of efficient reactions leading from simple starting materials to more complex species. This allows predictions of as yet unobserved cometary molecules. (2) Explanation of observed abundance and ratios, such as C_2H_6/CH_4 and HNC/HCN. (3) Investigation of low-albedo materials relevant for cometary nuclei (e.g., Halley and Borrelly). (4) Prediction of candidates for extended sources of CO, CN, H_2CO, and other molecules.

Here we describe some laboratory results related to the chemistry of ices in cometary nuclei, leaving comae chemistry for other chapters. The emphasis is on recent work, especially that providing insight into molecular evolution in comets.

4.1. Methods

Figure 11 represents a laboratory setup used to investigate cometary ice chemistry at the NASA Goddard Space Flight Center (GSFC). Similar equipment exists in other laboratories, with modifications made according to the interests of the investigators (e.g., *Allamandola et al.,* 1988; *Gerakines et al.,* 1996; *Demyk et al.,* 1998; *Strazzulla et al.,* 2001). In brief, the vacuum and temperature of outer space are simulated with a high-vacuum chamber and a cryostat respectively. An ice sample is formed on a precooled surface, to a thickness of a few micrometers or less, by condensation of room-temperature gases. The sample is then

TABLE 4. Estimated fluxes for ice processing environments, compared to laboratory experiments.

Environment (ice residence time in years)	Ion Processing			Photon Processing		
	Flux, 1 MeV p^+ (eV cm^{-2} s^{-1})	Energy absorbed (eV cm^{-2} s^{-1})*	Dose (eV $molecule^{-1}$)	Flux (eV cm^{-2} s^{-1})	Energy absorbed (eV cm^{-2} s^{-1})	Dose (eV $molecule^{-1}$)
Diffuse ISM (10^5–10^7)†	1×10^7	1.2×10^4	<1–30	9.6×10^8 at 10 eV†	5×10^8 0.02 μm ice	10^4–10^6
Dense cloud (10^5–10^7)†	1×10^6	1.2×10^3 0.02-μm ice	≪1–3	1.4×10^4 at 10 eV	1.7×10^3 0.02 μm ice	<1–4
Protoplanetary nebula (10^5–10^7)‡	1×10^6	1.2×10^3 0.02-μm ice	≪1–3	2×10^5 at 1–10 keV	§5 $\times 10^4$ 0.02 μm ice	2–240
Oort cloud (4.6×10^9)	φ(E)**	**	~150 (0.1 m) ~55–5 (1–5 m) <10 (5–15 m)	9.6×10^8 at 10 eV	9.6×10^8 0.1 μm ice	2.7×10^8
Laboratory (4.6×10^{-4})††	8×10^{16}	2×10^{15} 1-μm ice	10	2.2×10^{15} at 7.4 eV	2.2×10^{15} 1 μm ice	10

* The absorbed energy dose from 1-MeV cosmic-ray protons assumes a 300-MeV cm^2 g^{-1} stopping power and an H_2O-ice density of 1 g cm^{-3}. Protons deposit energy in both the entrance and exit ice layer of an ice-coated grain.

† 10 eV photons = 1200 Å, vacuum UV (UV-C). *Jenniskens et al.* (1993).

‡ Typical disk longevities (*Lawson et al.,* 1996).

§ Typical flux at 0.1 pc, 1 keV photons = 12 Å, soft X-rays (*Feigelson and Montmerle,* 1999).

¶ Absorbed energy dose from 1-keV X-rays assumes a 1-keV electron production in 1 g cm^{-3} H_2O-ice with a 127-MeV cm^2 g^{-1} stopping power.

** An energy dependent flux, φ(E), was used to calculate the resulting energy dose at different depths in a comet nucleus for an H_2O-ice density of 1 g cm^{-3}. For details see *Strazzulla and Johnson* (1991) and references therein.

†† Typical proton and UV data from the Cosmic Ice Laboratory at NASA Goddard.

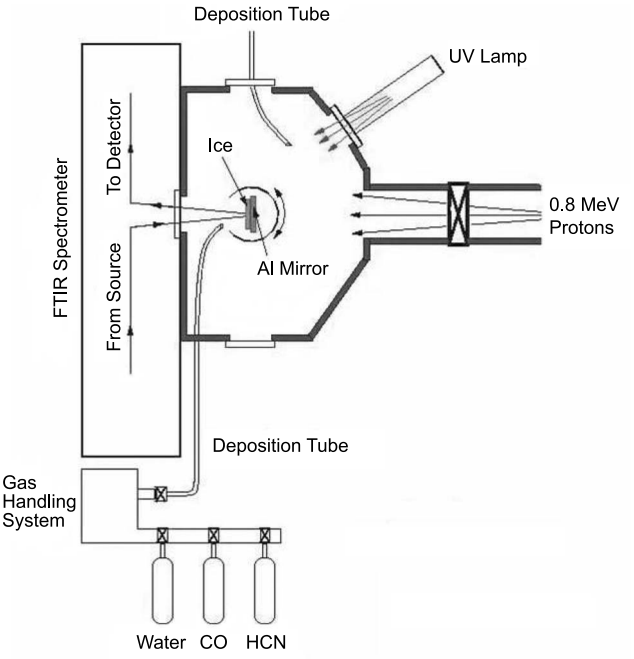

Fig. 11. Schematic of a laboratory setup for cometary ice experiments.

processed by positioning it before an ion beam to mimic cosmic-ray bombardment or a UV lamp to simulate far-UV exposure. The resulting ice chemistry can be followed by IR spectroscopy (see Fig. 11) or other techniques [e.g., UV (*Mennella et al.,* 1997), Raman (*Colangeli et al.,* 1992)]. At GSFC, a beam of ~1-MeV protons is generated by a Van de Graaff accelerator, while vacuum-UV photolysis is done with a flowing-H_2 microwave-discharge lamp (mostly 100–200-nm coverage).

To date, mid-IR spectroscopy (4000–400 cm^{-1}, 2.5–25 μm) has revealed more details of ice chemistry than any other laboratory method. Spectra in this region are from vibrations involving functional groups (groups of bonded atoms), with certain functional groups having very diagnostic absorbances. A disadvantage of IR spectroscopy is its relatively low sensitivity. Reaction products with low abundance can seldom be studied by IR alone, and often require a combination of chromatography and mass spectrometry for their identification during vaporization (e.g., *Bernstein et al.,* 1995).

4.2. Some Results and Case Histories

Of all cometary molecules, only H_2O has been detected in both the solid and gas phases (*Davies et al.,* 1997), all

other species having been observed only in gas-phase coma spectra. As H_2O is the most abundant nuclear molecule, it plays a particularly significant role in cometary ice chemistry. On exposure to either far-UV photons or high-energy (keV, MeV) ions, H_2O dissociates into H and OH radicals. Even at cometary and interstellar temperatures, H and OH can react with other molecules to produce many products.

Figure 12 summarizes an experiment in which an H_2O + CO (5 : 1) mixture was proton irradiated at 16 K (*Hudson and Moore,* 1999). Before the irradiation, none of the bands in the upper trace were present. The features shown were produced by radiolysis and can be identified, among other ways, by comparison to reference spectra. In each case, fragments from H_2O, either H or OH, form the products. For example, H-atom addition to CO along the sequence

$$CO \rightarrow HCO \rightarrow H_2CO \rightarrow CH_3O \text{ and/or}$$
$$CH_2OH \rightarrow CH_3OH$$

leads to H_2CO (formaldehyde) and CH_3OH (methanol), both being cometary molecules. Calculations of reaction yields are possible from a knowledge of intrinsic IR band strengths, and show that energetic processing can account for the known abundance of many cometary organics. In fact, radiolysis is presently the only process known to reproduce many observed abundances.

Formic acid, HCOOH, in Fig. 12 is particularly interesting as this molecule arises from *both* H and OH adding to CO, such as H-atom addition followed by OH reaction: C ≡ O → HC = O → HC(=O)OH. Since H_2O forms an isoelectronic series with NH_3 and CH_4, similar reactions will lead to $HC(=O)NH_2$, from NH_3 + CO, and $HC(=O)CH_3$, from CH_4 + CO. These products are indeed observed in the laboratory, and both are known cometary molecules.

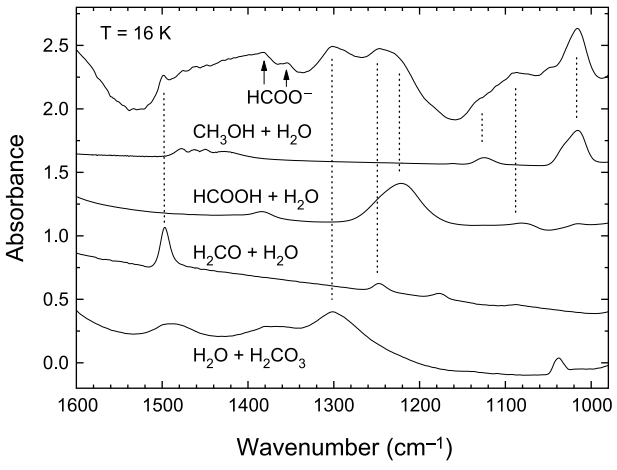

Fig. 12. New species formed in an H_2O + CO (5 : 1) ice irradiated to 11 eV molecule^{-1} are identified by comparison with reference spectra of dilute mixtures (H_2O : molecule > 5 : 1) at ~16 K. Spectra have been offset for clarity.

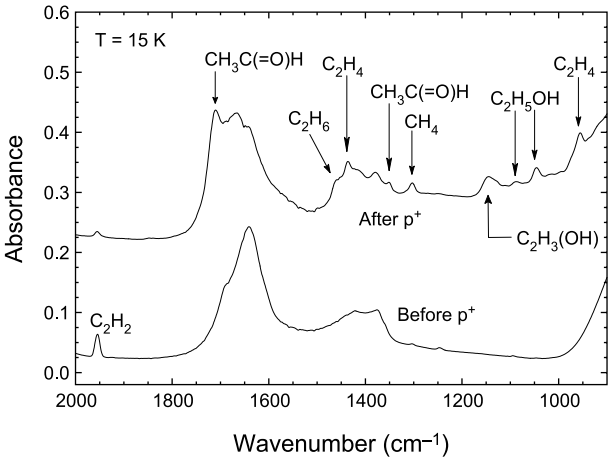

Fig. 13. Molecular synthesis in an H_2O + C_2H_2 (4 : 1) ice at 15 K after irradiation to a dose of 17 eV molecule^{-1}. Spectra have been offset for clarity.

Figure 13 shows a related experiment, a proton irradiation of an H_2O + C_2H_2 ice (4 : 1) at ~15 K (*Moore and Hudson,* 1998), work motivated by the discovery of C_2H_6 in Comet Hyakutake by *Mumma et al*. (1996). The upper trace gives identifications and, again, H- and OH-addition reactions explain most of the products. A quantitative analysis shows that this low-temperature ice chemistry can explain the unexpectedly high abundance of cometary C_2H_6.

Products from low-temperature reactions of known cometary molecules are summarized in Table 5 and represent work from various laboratories. The table is far from exhaustive [see *Cottin et al.* (1999) for a more complete listing]. Blanks in Table 5 indicate a lack of experimental data.

Experiments have also revealed the radiolysis and photolysis products of many single-component ices, and a summary is provided in Table 6, which is again far from exhaustive. Yields for some of these products may be low in the H_2O-rich ices of comets, but enrichment of the less-volatile materials may occur as highly volatile species are lost over many cometary apparitions. This effect is manifested in the laboratory by a room-temperature residue that remains after processed ices are warmed under vacuum. These residues are the subject of much interest, as chromatographic analyses show that they contain high molecular weight compounds. In residues from more complex ices, biomolecules, such as certain amino acids, are found in trace amounts (e.g., *Bernstein et al.,* 2002). These materials are thought to accumulate on cometary nuclei where they may have been delivered to the early Earth. If such molecules survived impact they could have significantly enhanced the variety and volume of the Earth's chemical inventory. In both single- and multicomponent ice experiments, residual materials are also of interest as they could explain the extended sources of H_2CO, CN, CO, and other molecules seen in comae.

TABLE 5. Products from reactions of H_2O-dominated two-component ices at 10–20 K (references given in brackets).

Mixture	Reaction Products Identified	Processing
$H_2O + CO$	CO_2, HCO, H_2CO (+ CH_3OH, HCOOH, $HCOO^-$, H_2CO_3 from ion expts.)	Ion [1], UV [2]
$H_2O + CO_2$	CO, H_2CO_3, O_3, H_2O_2	Ion [3,4], UV [4,5]
$H_2O + CH_4$	CH_3OH, C_2H_5OH, C_2H_6, CO, CO_2	Ion [6]
$H_2O + C_2H_2$	C_2H_5OH, CH_3OH, C_2H_6, C_2H_4, CO, CO_2, CH_4, C_3H_8, $HC(=O)CH_3$, $CH_2CH(OH)$	Ion [6], UV [7]
$H_2O + C_2H_6$	CH_4, C_2H_4, CH_3CH_2OH,CO, CO_2, CH_3OH	Ion [8]
$H_2O + H_2CO$	CO_2, CO, CH_3OH, HCO, HCOOH, CH_4	Ion [1]
$H_2O + CH_3OH$	CO, CO_2, H_2CO, HCO, CH_4, (+ $C_2H_4(OH)_2$, $HCOO^-$ from ion expts.)	Ion [9,10], UV [2]
$H_2O + NH_3$	[none reported]	Ion [11]
$H_2O + HCN$	CN^-, HNCO, OCN^-, $HC(=O)NH_2$, NH_4^+ (?), CO, CO_2	Ion [8,12]
$H_2O + HNCO$	NH_4^+, OCN^-, CO, CO_2	UV [8]
$H_2O + HCOOH$	CO, CO_2, H_2CO	Ion [8]
$H_2O + HC(=O)CH_3$	CO_2, CO, CH_4, CH_3CH_2OH	Ion [8]
$H_2O + HC(=O)NH_2$	CO, CO_2, HNCO, OCN^-	UV [8,12]
$H_2O + HC(=O)OCH_3$	CO_2, CO, H_2CO, CH_3OH, CH_4	Ion [8], UV [8]
$H_2O + SO_2$		
$H_2O + H_2S$	S_2	UV [13]
$H_2O + OCS$	CO, CO_2, SO_2, H_2CO (?), H_2O_2 (?)	Ion [8]
$H_2O + CH_3CN$	H_2CCNH, CH_4, OCN^-, CN^-	Ion [8,12]
$H_2O + HCCCN$		

References: [1] *Hudson and Moore* (1999); [2] *Allamandola et al*. (1988); [3] *Brucato et al.* (1997); [4] *Gerakines et al*. (2000); [5] *Wu et al.* (2003); [6] *Moore and Hudson* (1998); [7] *Wu et al.* (2002); [8] M. H. Moore et al. (unpublished work, 2003); [9] *Hudson and Moore* (2000); [10] *Palumbo et al*. (1999); [11] *Strazzulla and Palumbo* (1998); [12] *Hudson et al*. (2001); [13] *Grim and Greenberg* (1987a).

TABLE 6. Products from reactions of one-component ices at 10–20 K (references given in brackets).

Ice	Reaction Products Identified	Least-Volatile Species	Processing Experiment
H_2O	H_2O_2, HO_2 [2], OH [2]	H_2O_2	Ion [1], UV [2]
CO	CO_2, C_3O_2, C_2O	C_3O_2	Ion [3], UV [2]
CO_2	CO, O_3, CO_3	H_2CO_3 (from H^+ implantation) [4]	Ion [3,4], UV [1,2]
CH_4	C_2H_2, C_2H_4, C_2H_6, C_3H_8, CH_3, C_2H_5	PAHs [5] and high molecular weight hydrocarbons	Ion [5–7], UV [2]
C_2H_2	CH_4 [6], polyacetylene [8]	PAHs [5], polyacetylene [8]	Ion [5,8]
C_2H_6			
H_2CO	POM, CO, CO_2, HCO	POM	Ion [8], UV [2]
CH_3OH	CH_4, CO, CO_2, H_2CO, H_2O, $C_2H_4(OH)_2$, HCO, $HCOO^-$	$C_2H_4(OH)_2$	Ion [9,10], UV [2]
NH_3	N_2H_4 [2], NH_2 [2]	N_2H_4 [2]	Ion [12], UV [2]
HCN	HCN oligomers	HCN oligomers	Ion [8], UV [8]
HNCO	NH_4^+, OCN^-, CO, CO_2	NH_4OCN	Ion [8], UV [8]
HCOOH			
$HC(=O)CH_3$			
$HC(=O)NH_2$			
$HC(=O)OCH_3$			
SO_2	SO_3	S_8 [12]	Ion [12], UV [13]
H_2S	none reported		UV [13]
OCS			
CH_3CN	CH_4, H_2CCNH, CH_3NC		Ion [8], UV [8]
HCCCN			

References: [1] *Moore and Hudson* (2000); [2] *Gerakines et al*. (1996); [3] *Gerakines and Moore* (2001); [4] *Brucato et al*. (1997); [5] *Kaiser and Roessler* (1998); [6] *Mulas et al.* (1998); [7] *Moore and Hudson* (2003); [8] M. H. Moore et al. (unpublished work, 2003); [9] *Hudson and Moore* (2000); [10] *Palumbo et al*. (1999); [11] *Strazzulla and Palumbo* (1998); [12] *Moore* (1984); [13] *Salama et al.* (1990).

Laboratory work also suggests ions as likely chemical components of comets. Both radiolysis and photolysis of cometary ice analogs readily generate acids which, if NH_3 is present, undergo proton-transfer reactions of the type

$$HX + NH_3 \rightarrow X^- + NH_4^+$$

to produce stable ions. These ions would accumulate on the surface of a comet nucleus, or anywhere that sufficient energetic processing occurs. Figure 14 illustrates this type of acid-base chemistry, where the upper spectrum is from the irradiated H_2O + CO (5 : 1) mixture of Fig. 12, while the lower spectrum is from an irradiated $H_2O + CO + NH_3$ (5:1:1) mixture (*Hudson et al.,* 2001). The $HCOO^-$ (formate) and NH_4^+ (ammonium) ion positions are indicated by arrows, and demonstrate that acid-base chemistry has occurred. Other ions that have been studied are OCN^- (*Grim and Greenberg,* 1987b; *Hudson et al.,* 2001) and CN^- (*Moore and Hudson,* 2003). H_3O^+ and OH^- also are likely in cometary nuclei, but difficult to detect by IR methods as they lack strong unobscured bands.

Not only have changes in ice composition been investigated in the laboratory, but changes in ice phase have been studied (*Baratta et al.,* 1991). Crystalline H_2O-ice can be converted into amorphous ice by either ionizing radiation or UV photons (*Leto and Baratta,* 2003). This amorphization is a general phenomenon and, at least for H_2O and CH_3OH, occurs with a rate that varies inversely with temperature (*Hudson and Moore,* 1995). Amorphization experiments also are related to the question of cometary clathrate hydrates, crystalline cage-like solids. Laboratory work shows that the H_2O-CH_3OH clathrate is readily destroyed by radiation, raising serious questions about the stability of clathrates in cometary ice (*Hudson and Moore,* 1993).

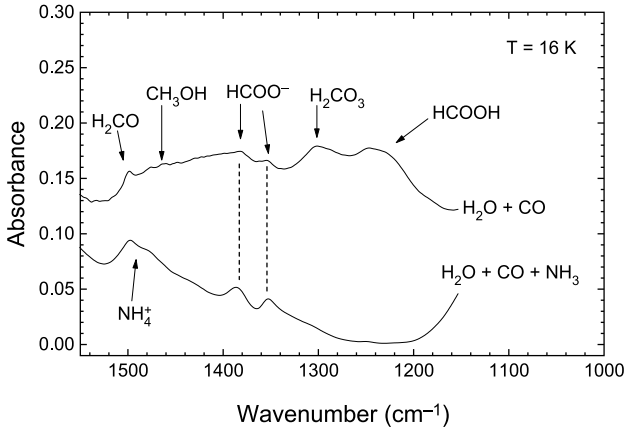

Fig. 14. Infrared spectra of two irradiated laboratory ices at 16 K, showing the influence of acid-base chemistry. The upper trace is an H_2O + CO (5 : 1) ice and the lower trace is an H_2O + CO + NH_3 (5 : 1 : 1) ice. Both were irradiated to about 25 eV molecule^{-1}.

Finally, we mention one of the most persistent puzzles of cometary chemistry, the extraordinarily dark color of the nuclei of Comet Halley and Comet Borrelly. The most reasonable explanation for low nuclear albedos is that radiolysis of cometary organics and CO produced a dark C-rich material that accumulated over time (*Johnson et al.,* 1987). However, experiments showing progressive carbonization in H_2O-rich ices are lacking. More experiments and data-based chemical models are needed.

To summarize and conclude this section, laboratory experiments have revealed efficient condensed-phase syntheses for many cometary molecules such as H_2CO, CH_3OH, HCOOH, C_2H_6, $HC(=O)NH_2$, and $HC(=O)CH_3$, as discussed. Reactions to make other molecules, such as CO_2 and HNCO, have also been studied (*Hudson et al.,* 2001). Understanding the formation paths to other volatiles, and how they might relate to the dark nuclear surface, is work in progress.

4.3. Future Steps

Little has been published on the ice chemistry of molecules containing either a cyanide (CN) group or sulfur, two types of interest to astrobiologists. Cometary cyanides include H-CN, H_3C-CN, and HC ≡ C-CN. The corresponding isocyanides are known in the interstellar medium, but only H-NC has been reported in comets. Both the formation and abundance of HCN and HNC, and their ratio of HNC/HCN ~ 0.1, are of much interest, but lack a full explanation (*Rodgers and Charnley,* 2001). Cyanide isomerizations seen in the laboratory suggest new cometary molecules awaiting detection, such as H_3C-NC and HC ≡ C-NC from H_3C-CN and HC ≡ C-CN, respectively, and $H_2C = C =$ NH from H_3C-CN. Also, a sequence similar to HC ≡ CH → $H_2C = CH_2 \rightarrow H_3C$-$CH_3$ may apply to HC ≡ C-CN, giving cometary H_2C = CH-CN and H_3C-CH_2-CN, but more laboratory work is needed for a firmer prediction. As for sulfur, it is present in comets as H_2CS, H_2S, OCS, SO_2, and other species. An observational search for CH_3SH is suggested, as CH_3SH could be formed from H_2CS in analogy with the $H_2CO \rightarrow CH_3OH$ reaction. More laboratory work on cometary sulfur chemistry certainly is needed, as evidenced by the gaps in Tables 5 and 6. For some early work on sulfur ice chemistry, see *Grim and Greenberg* (1987a).

Other new molecules recommended for searches, based on experiments, include ethanol (*Moore and Hudson,* 1998), ethylene glycol (*Hudson and Moore,* 2000), and vinyl alcohol (*Hudson and Moore,* 2003), all readily formed by ice processing. Acetic acid, glycolaldehyde, vinyl alcohol, and ethylene oxide, all detected in the interstellar medium, are probably cometary molecules as well, and isomers of each are seen in coma spectra.

Future laboratory work will undoubtedly include the roles of interstellar grains in ice chemistry. Do grains simply provide an inert reaction template or are they a catalytic surface? Much surface chemistry remains to be done on

cometary and interstellar molecules, and impressive experiments are already being published (*Fraser et al.,* 2002).

5. CONCLUSIONS AND OUTLOOK

The results described in this chapter demonstrate the great value of laboratory simulations of cometary materials and processes. Progress in laboratory experiments has grown in parallel to the increase of information from cometary observations and the reliability of models describing solar system formation and the role played by comets. This chapter demonstrates that laboratory results are needed to understand the composition and evolution of both cometary nuclei and comae, and to provide guidelines for future exploration and model development. This is true for both refractory and ice components of comets.

Nevertheless, uncertainties remain and the field of research using laboratory experiments is rich with new tasks to accomplish. Generally speaking, the characterization of ice and dust analogs must continue to move in the direction of using complementary techniques, mainly *in situ* methods, applied during or immediately after sample production and/or treatment. Only in this way can information on the different factors that characterize materials, and their possible counterparts in real space conditions, be determined. New methods are also needed to produce samples with compositional and structural properties that can be selected by controllable parameters. In this respect, a new approach in laboratory experiments concerns *mixtures* of various refractory compounds (e.g., silicates and carbons) and of refractory and icy species. It is expected that results from this approach will offer a drastic change of perspective in the interpretation of observations.

As for refractory compounds, the study of silicate (amorphous vs. crystalline) structure and detailed composition (e.g., cation relative abundance) vs. space environment conditions is a key problem that extends over a cosmic scale, including material formation around cold stars, processing in the diffuse and dense ISM, and evolution during solar system formation. In this framework the role of silicate hydration is a subject that deserves particular attention in the future. Similarly, problems connected to carbonaceous grains also are important due to the strong connections to the evolution of C-based (large and small) molecular species. We now know that comets contain condensed organics and C grains (CHON particles), but the routes of formation and the connections among these two populations of compounds are still uncertain. To gain insight into this problem, a careful consideration is needed of how and when these compounds were formed in the circumstellar/interstellar media, and how they evolved until and after comet formation.

Concerning icy materials, section 4.3 above outlines some needed work, and the gaps in Tables 5 and 6 are obvious. A combination of small- and large-scale experiments is probably the correct approach for tracing the physical and chemical evolution of cometary bodies. The most reasonable way to understand and predict the actual behavior of comets, pre- and postperihelion, appears to start with an understanding of chemical reaction paths and to continue on through the identification of phenomena that affect the behavior of comet nuclei as a whole.

In conclusion, the aim of laboratory experiments is to increase our knowledge of how chemical species, at various levels and in different forms of arrangement, evolve in space. Laboratory scientists are encouraged to carry on their programs as the astrophysical community now recognizes that interpretations of cosmic evolution, comets included, cannot proceed without the firm reference frame offered by laboratory results.

Acknowledgments. The experimental work at INAF – Osservatorio Astronomico di Capodimonte is partially supported by contracts from ASI and MIUR. The research at Tel-Aviv University was supported by the Deutche Forschungs – Gemeinschaft, the Israel Science foundation (Grant 194/93-2), and the United States – Israel Bi-national Science Foundation (Grant 2000005). Work at NASA Goddard Space Flight Center was supported through NASA's Laboratory for Planetary Atmospheres and Space Astrophysics Research and Analysis programs.

REFERENCES

Allamandola L. J., Sandford S. A., and Valero G. J. (1988) Photochemical and thermal evolution of interstellar/precometary ice analogs. *Icarus, 76,* 225–252.

Allamandola L. J., Tielens A. G. G. M., and Herbst T. M. (1993) Diamonds in dense molecular clouds — A challenge to the standard interstellar medium paradigm. *Science, 260,* 64–66.

Bar-Nun A. and Laufer D. (2003) First experimental studies of large samples of gas-laden amorphous "cometary" ices. *Icarus, 161,* 157–163.

Bar-Nun A., Herman G., Laufer D., and Rappaport M. L. (1985) Trapping and release of gases by water ice and implications for icy bodies. *Icarus, 63,* 317–332.

Bar-Nun A., Dror J., Kochavi E., and Laufer D. (1987) Amorphous water ice and its ability to trap gases. *Phys. Rev. B., 35,* 2427–2435.

Baratta G. A., Spinella F., Leto G., Strazzulla G., and Foti G. (1991) The 3.1 μm feature in ion-irradiated water ice. *Astron. Astrophys., 252,* 421–424.

Baratta G. A., Mennella V., Brucato J. R., Colangeli L., Leto G., Palumbo M. E., and Strazzulla G. (2004) Raman spectroscopy of ion irradiated interplanetary carbon dust analogues. *J. Raman Spectroscopy,* in press.

Benkhoff J. and Spohn T. (1991) Thermal histories of the KOSI samples. *Geophys. Res. Lett., 18,* 261–264.

Bernstein M. P., Sandford S. A., Allamandola L. J., and Chang S. (1995) Organic compounds produced by photolysis of realistic interstellar and cometary ice analogs containing methanol. *Astrophys. J., 454,* 327–344.

Bernstein M. P., Dworkin J. P., Sandford S. A., Cooper G. W., and Allamandola L. J. (2002) Racemic amino acids from the ultraviolet photolysis of interstellar ice analogues. *Nature, 416,* 401–401.

Bertie J. E. and Devlin J. P. (1983) Infrared spectroscopic proof of

the formation of the structure I hydrate of oxirane from annealed low-temperature condensate. *J. Chem. Phys., 78,* 6340–6341.

Biver N. and 22 colleagues (1999) Long-term evolution of the outgassing of comet Hale-Bopp from radio observations. *Earth Moon Planets, 78,* 5–11.

Blake D., Allamandola L., Sandford S., Hudgins D., and Freund F. (1991) Clathrate hydrate formation in amorphous cometary ice analogs in vacuo. *Science, 254,* 548–551.

Bockelée-Morvan D., Gautier D., Lis D. C., Young K., Keene J., Phillips T., Owen T., Crovisier J., Goldsmith P. F., Bergin E. A., Despois D., and Wootten A. (1998) Deuterated water in comet C/1996 B2 (Hyakutake) and its implications for the origin of comets. *Icarus, 133,* 147–162.

Bockelée-Morvan D., Gautier D., Hersant F., Huré J. M., and Robert F. (2002) Turbulent radial mixing in the solar nebula as the source of crystalline silicates in comets. *Astron. Astrophys., 384,* 1107–1118.

Bockelée-Morvan D., Crovisier J., Mumma M. J., and Weaver H. A. (2004) The composition of cometary volatiles. In *Comets II* (M. C. Festou et al., eds.) this volume. Univ. of Arizona, Tucson.

Bohren C. F. and Huffman D. R. (1983) *Absorption and Scattering of Light by Small Particles.* Wiley, New York. 544 pp.

Brinker C. J. and Scherer G. W. (1990) *Sol-Gel Science: The Physics and Chemistry of Sol-Gel Processing.* Academic, San Diego. 912 pp.

Brownlee D. E., Pilachowski L., Olszewski E., and Hodge P. W. (1980) Analysis of interplanetary dust collections. In *Solid Particles in the Solar System* (I. Halliday, ed.), pp. 333–341. Reidel, Dordrecht.

Brucato J., Palumbo M. E., and Strazzulla G. (1997) Carbonic acid by ion implantation in water/carbon dioxide ice mixtures. *Icarus, 125,* 135–144.

Brucato J. R., Colangeli L., Mennella V., Palumbo P., and Bussoletti E. (1999a) Mid-infrared spectral evolution of thermally annealed amorphous pyroxene. *Astron. Astrophys., 348,* 1012–1019.

Brucato J. R., Colangeli L., Mennella V., Palumbo P., and Bussoletti E. (1999b) Silicates in Hale-Bopp: Hints from laboratory studies. *Planet. Space Sci., 47,* 773–779.

Brucato J. R., Mennella V., Colangeli L., Rotundi A., and Palumbo P. (2002) Production and processing of silicates in laboratory and in space. *Planet. Space Sci., 50,* 829–837.

Campins H. and Ryan E. V. (1989) The identification of crystalline olivine in cometary silicates. *Astrophys. J., 341,* 1059–1066.

Chiar J. E., Pendleton Y. J., Geballe T. R., and Tielens A. G. G. M. (1998) Near-infrared spectroscopy of the proto-planetary nebula CRL 618 and the origin of the hydrocarbon dust component in the interstellar medium. *Astrophys. J., 507,* 281–286.

Chyba C. F. (1987) The cometary contribution to the oceans of primitive Earth. *Nature, 330,* 632–635.

Chyba C. F. (1990) Impact delivery and erosion of planetary oceans in the inner solar system. *Nature, 343,* 129–133.

Cochran A. L. (2002) A search for N_2^+ in spectra of comet C/2002 C1 (Ikeya-Zhang). *Astrophys. J. Lett., 576,* L165–L168.

Cochran A. L., Cochran W. D., and Barker E. B. (2000) N_2^+ and CO^+ in Comets 122P/1995 S1 (de Vico) and C/1995 O1 (Hale-Bopp). *Icarus, 146,* 583–593.

Colangeli L., Mennella V., Baratta G. A., Bussoletti E., and Strazzulla G. (1992) Raman and infrared spectra of polycyclic aromatic hydrocarbon molecules of possible astrophysical interest. *Astrophys. J., 396,* 369–377.

Colangeli L., Mennella V., di Marino C., Rotundi A., and Bussoletti E. (1995) Simulation of the cometary 10 μm band by means of laboratory results on silicatic grains. *Astron. Astrophys., 293,* 927–934.

Colangeli L., Mennella V., Rotundi A., Palumbo P., and Bussoletti E. (1996) Simulation of the cometary 10 micron band by laboratory data. II. Extension to spectra available for different comets. *Astron. Astrophys., 312,* 643–648.

Colangeli L. and 20 colleagues (2003) The role of laboratory experiments in the characterisation of silicon-based cosmic material. *Astron. Astrophys. Rev., 11,* 97–152.

Cottin H., Gazeau M. C., and Raulin F. (1999) Cometary organic chemistry: A review from observations, numerical and experimental simulations. *Planet. Space Sci., 47,* 1141–1162.

Crovisier J. (1999) Infrared observations of volatile molecules in comet Hale-Bopp. *Earth Moon Planets, 79,* 125–143.

Crovisier J., Leech K., Bockelée-Morvan D., Brooke T. Y., Hanner M. S., Altieri B., Keller H. U., and Lellouch E. (1997) The spectrum of Comet Hale-Bopp (C/1995 O1) observed with the Infrared Space Observatory at 2.9 AU from the Sun. *Science, 275,* 1904–1907.

Davies J. K., Puxley P. J., Mumma M. J., Reuter D. C., Hoban S., Weaver H. A., and Lumsden S. L. (1993) The infrared (3.2–3.6 micron) spectrum of comet P/Swift-Tuttle — Detection of methanol and other organics. *Mon. Not. R. Astron. Soc., 265,* 1022–1993.

Davies J. K., Roush T. L., Cruikshank D. P., Bartholemew M. J., Geballe T. R., Owen T., and de Bergh C. (1997) The detection of water ice in comet Hale-Bopp. *Icarus, 127,* 238–245.

Demyk K., Dartois E., d'Hendecourt L., Jourdain de Muizon M., Heras A. M., and Breitfellner M. (1998) Laboratory identification of the 4.62 μm solid state absorption band in the ISO-SWS spectrum of RAFGL 7009S. *Astron. Astrophys., 339,* 553–560.

Despois D. (1997) Radio observation of molecular and isotopic species: Implications on the interstellar origin of cometary ices. *Earth Moon Planets, 79,* 103–124.

Dones L., Weissman P. R., Levison H. F., and Duncan M. J. (2004) Oort cloud formation and dynamics. In *Comets II* (M. C. Festou et al., eds.), this volume. Univ. of Arizona, Tucson.

Eberhardt P., Reber M., Krankowsky D., and Hodges R. R. (1995) The D/H and $^{18}O/^{16}O$ ratios in water from comet P/Halley. *Astron. Astrophys., 302,* 301–318.

Ehrenfreund P., Charnley S. B., and Wooden D. (2004) From interstellar material to comet particles and molecules. In *Comets II* (M. C. Festou et al., eds.), this volume. Univ. of Arizona, Tucson.

Engel S., Lunine J. I., and Lewis J. S. (1990) Solar nebula origin for volatile gases in Halley's comet. *Icarus, 85,* 380–393.

Fabian D., Jäger C., Henning Th., Dorschner J., and Mutschke H. (2000) Steps toward interstellar silicate mineralogy. V. Thermal evolution of amorphous magnesium silicates and silica. *Astron. Astrophys., 364,* 282–292.

Farnham T. L. and Cochran A.L. (2002) A McDonald observatory study of comet 19P/Borrelly: Placing the Deep Space 1 observations into a broader context. *Icarus, 160,* 398–418.

Feigelson E. D. and Montmerle T. (1999) High-energy processes in young stellar objects. *Annu. Rev. Astron. Astrophys., 37,* 363–408.

Fraser H. J., Collings M. P., and McCoustra M. R. S. (2002) Laboratory surface astrophysics experiment. *Rev. Sci. Instrum., 73,* 2161–2170.

Gerakines P. A. and Moore M. H. (2001) Carbon suboxide in

astrophysical ice analogs. *Icarus, 154,* 372–380.
Gerakines P. A., Schutte W. A., and Ehrenfreund P. (1996) Ultraviolet processing in interstellar ice analogs: I. Pure ices. *Astron. Astrophys., 312,* 289–305.
Gerakines P. A., Moore M. H., and Hudson R. L. (2000) Carbonic acid production in $H_2O:CO_2$ ices. UV photolysis vs. proton bombardment. *Astron. Astrophys., 357,* 793–800.
Goldreich P. and Ward W. R. (1973) The formation of planetesimals. *Astrophys. J., 183,* 1051–1062.
Green J. R. and Bruesch L. S. (2000) Laboratory simulation of cometary nuclei: Mechanical properties of porous ice-dust mixtures. *Bull. Am. Astron. Soc., 32,* 1061.
Green J. R., Bruesch L. S., Oakes R., Pinkham B., and Folsom C. L. (1999) Comet simulation experiments at JPL. *Bull. Am. Astron. Soc., 31,* 1589.
Greenberg J. M. and Hage J. I. (1990) From interstellar dust to comets — A unification of observational constraints. *Astrophys. J., 361,* 260–274.
Grim R. J. A. and Greenberg J. M. (1987a) Photoprocessing of H_2S in interstellar grain mantles as an explanation for S2 in comets. *Astron. Astrophys., 181,* 155–168.
Grim R. J. A. and Greenberg J. M. (1987b) Ions in grain mantles — The 4.62 micron absorption by OCN(–) in W33A. *Astrophys. J. Lett., 321,* L91–L96.
Grün E., Bar-Nun A., Benkhoff J., Bischoff A., Düren H., Hellman H., Hesselbarth P., Hsiung P., Keller H. U., Klinger J., Knölker J., Kochan H., Kohl H., Kölzer G., Krankowsky D., Lämmerzahl P., Mauersberger K., Neukum G., Öhler A., Ratke L., Rössler K., Schwehm G., Spohn T., Stöffler D., and Thiel K. (1991) Laboratory simulation of cometary processes: Results from first KOSI experiments. In *Comets in the Post-Halley Era* (R. L. Newburn et al., eds.), pp. 277–297. Kluwer, Dordrecht.
Gustafson B. Å S. (1996) Microwave analog to light scattering measurements: A modern implementation of a proven method to achieve precise control. *J. Quant. Spectrosc. Radiat. Transfer, 55,* 663–672.
Hadamcik E., Renard J. B., Worms J. C., Levasseur-Regourd A. C., and Masson M. (2002) Polarization of light scattered by fluffy particles (PROGRA^2 experiment). *Icarus, 155,* 497–508.
Hallenbeck S. L., Nuth J. A., and Daukantas P. L. (1998) Mid-infrared spectral evolution of amorphous magnesium silicate smokes annealed in vacuum: Comparison to cometary spectra. *Icarus, 131,* 198–209.
Hallenbeck S. L., Nuth J. A. III, and Nelson R. N. (2000) Evolving optical properties of annealing silicate grains: From amorphous condensate to crystalline mineral. *Astrophys. J., 535,* 247–255.
Hanner M. S. and Bradley J. P. (2004) Composition and mineralogy of cometary dust. In *Comets II* (M. C. Festou et al., eds.), this volume. Univ. of Arizona, Tucson.
Hanner M. S., Lynch D. K., and Russell R. W. (1994) The 8–13 micron spectra of comets and the composition of silicate grains. *Astrophys. J., 425,* 274–285.
Harker D. E. and Desch S. J. (2002) Annealing of silicate dust by nebular shocks at 10 AU. *Astrophys. J. Lett., 565,* L109–L112.
Harker D. E., Wooden D. H., Woodward C. E., and Lisse C. M. (2002) Grain properties of comet C/1995 O1 (Hale-Bopp). *Astrophys. J., 580,* 579–597.
Hayward T. L. and Hanner M. S. (1997) Spectrocam-10 thermal infrared observations of the dust in comet C/1995 O1 Hale-Bopp. *Earth Moon Planets, 78,* 265–270.
Hilchenbach M., Kochemann O., and Rosenbauer H. (2000) Impact on a comet: Rosetta Lander simulations. *Planet. Space Sci., 48,* 361–369.
Hovenier J.W. and van der Mee C. V. M. (2000) Measuring scattering matrices of small particles at optical wavelengths. In *Light Scattering by Non-Spherical Particle*s (M. I. Mishchenko et al., eds.), pp. 61–85. Academic, San Diego.
Hudson R. L. and Donn B. (1991) An experimental study of the sublimation of water ice and the release of trapped gases. *Icarus, 94,* 326–332.
Hudson R. L. and Moore M. H. (1993) Far-infrared investigations of a methanol clathrate hydrate: Implications for astronomical observations. *Astrophys. J. Lett., 404,* L29–L32.
Hudson R. L. and Moore M. H. (1995) Far-IR spectral changes accompanying proton irradiation of solids of astrochemical interest. *Radiat. Phys. Chem., 45,* 779–789.
Hudson R. L. and Moore M. H. (1999) Laboratory studies of the formation of methanol and other organic molecules by water + carbon monoxide radiolysis: Relevance to comets, icy satellites, and interstellar ices. *Icarus, 140,* 451–461.
Hudson R. L. and Moore M. H. (2000) IR spectra of irradiated cometary ice analogues containing methanol: A new assignment, a reassignment, and a non-assignment. *Icarus, 145,* 661–663.
Hudson R. L. and Moore M. H. (2003) Solid-phase formation of interstellar vinyl alcohol. *Astrophys J. Lett., 586,* L107–L110.
Hudson R. L., Moore M. H. and Gerakines P. A. (2001) The formation of cyanate ion (OCN^-) in interstellar ice analogues. *Astrophys. J., 550,* 1140–1150.
Irvine W. M., Schloerb F. P., Crovisier J., Fegley B., and Mumma M. J. (2000) Comets: A link between interstellar and nebular chemistry. In *Protostars and Planets IV* (V. Mannings et al., eds.), p. 1159. Univ. of Arizona, Tucson.
Jäger C., Dorschner J., Mutschke,H., Posch Th., and Henning Th. (2003) Steps toward interstellar silicate mineralogy. VII. Spectral properties and crystallization behaviour of magnesium silicates produced by the sol-gel method. *Astron. Astrophys., 408,* 193–204.
Jenniskens P. and Blake D. F. (1994) Structural transitions in amorphous water ice and astrophysical implications. *Science, 265,* 753–756.
Jenniskens P. and Blake D. F. (1996) Crystallization of amorphous water ice in the solar system. *Astrophys. J., 473,* 1104–1113.
Jenniskens P., Baratta G. A., Kouchi A., deGroot M. S., Greenberg J. M., and Strazzulla G. (1993) Carbon dust formation on interstellar grains. *Astron. Astrophys., 273,* 583–600.
Jenniskens P., Blake D. F., Wilson M. A., and Pohorille A. (1995) High density amorphous ice, the frost on interstellar grains. *Astrophys. J., 455,* 389–401.
Jenniskens P., Banham S. F., Blake D. F., and McCoustra M. R. S. (1997) Liquid water in the domain of cubic crystalline ice IC. *J. Chem. Phys., 107,* 1232–1241.
Jessberger H. L. and Kotthaus M. (1989) Compressive strength of synthetic comet nucleus samples. In *Proceedings of an International Workshop on the Physics and Mechanics of Cometary Materials* (J. Hunt and T. D. Guyenne, eds.), pp. 141–146. ESA SP-302, Noordwijk, The Netherlands.
Johnson R. E., Cooper J. F., Lanzerotti L. J., and Strazzulla G. (1987) Radiation formation of a non-volatile comet crust. *Astron. Astrophys., 187,* 889–892.
Kaiser R. I. and Roessler K. (1998) Theoretical and laboratory studies on the interaction of cosmic-ray particles with interstellar ices. III. Suprathermal chemistry-induced formation of hydrocarbon molecules in solid methane, (CH_4), ethylene

(C_2H_4), and acetylene (C_2H_2). *Astrophys. J., 503,* 959–975.

Kawakita H. and 18 colleagues (2001) The spin temperature of NH_3 in comet C/1999S4 (LINEAR). *Science, 294,* 1089–1091.

Keller H. U., Britt D., Buratti B. J., and Thomas N. (2004) In situ observations of cometary nuclei. In *Comets II* (M. C. Festou et al., eds.), this volume. Univ. of Arizona, Tucson.

Klinger J. (1980) Influence of a phase transition of ice on the heat and mass balance of comets. *Science, 209,* 271–272.

Köster H. M. (1979) *Die chemische Silikatanalyse.* Springer-Verlag, Berlin.

Kouchi A. and Sirono S. (2001) Crystallization heat of impure amorphous H_2O ice. *Geophys. Res. Lett., 28,* 827–830.

Kouchi A., Greenberg J. M., Yamamoto T., and Mukai T. (1992) Extremely low thermal conductivity of amorphous ice — Relevance to comet evolution. *Astrophys. J. Lett., 388,* L73–L76.

Laufer D., Kochavi E., and Bar-Nun A. (1987) Structure and dynamics of amorphous water ice. *Phys. Rev. B, 36,* 9219–9227.

Laufer D., Notesco G., Bar-Nun A., and Owen T. (1999) From the interstellar medium to Earth's oceans via comets — an isotopic study of HDO/H_2O. *Icarus, 140,* 446–450.

Lawson W. A., Feigelson E. D., and Huenemoerder D. P. (1996) An improved HR diagram for Chamaeleon I pre-main-sequence stars. *Mon. Not. R. Astron. Soc., 280,* 1071–1088.

Leto G. and Baratta G. A. (2003) Ly-alpha photon induced amorphization of Ic water ice at 16 K. Effects and quantitative comparison with ion irradiation. *Astron. Astrophys., 397,* 7–13.

Levasseur-Regourd A. C., Hadamcik E., and Renard J. B. (1996) Evidence for two classes of comets from their polarimetric properties at large phase angles. *Astron. Astrophys., 313,* 327–333.

Lumme K., Rahola J., and Hovenier J. W. (1997) Light scattering by dense clusters of spheres. *Icarus, 126,* 455–469.

Lunine J. I. (1989) Primitive bodies — Molecular abundances in Comet Halley as probes of cometary formation environments. In *The Formation and Evolution of Planetary Systems* (H. A. Weaver and L. Danly, eds.), pp. 213–238. Cambridge Univ., Cambridge.

Marfunin A. S. (1995) *Methods and Instrumentations: Results and Recent Developments.* Springer-Verlag, New York. 441 pp.

Mauersberger K., Michel H. J., Krankowsky D., Laemmerzahl P., and Hesselbarth P. (1991) Measurement of the volatile component in particles emitted from an ice/dust mixture. *Geophys. Res. Lett., 18,* 277–280.

Meier R., Owen T. C., Jewitt D. C., Matthews H. E., Senay M., Biver N., Bockelée-Morvan D., Crovisier J., and Gautier D. (1998) Deuterium in comet C/1995 O1 (Hale-Bopp): Detection of DCN. *Science, 279,* 1707–1710.

Melosh H. J. and Vickery A. M. (1989) Impact erosion of the primordial atmosphere of Mars. *Nature, 338,* 487–489.

Mennella V., Colangeli L., Blanco A., Bussoletti E., Fonti S., Palumbo P., and Mertins H. C. (1995) A dehydrogenation study of cosmic carbon analogue grains. *Astrophys. J., 444,* 288–292.

Mennella V., Colangeli L., Palumbo P., Rotundi A., Schutte W., and Bussoletti E. (1996) Activation of an ultraviolet resonance in hydrogenated amorphous carbon grains by exposure to ultraviolet radiation. *Astrophys. J. Lett., 464,* L191–L194.

Mennella V., Baratta G. A., Colangeli L., Palumbo P., Rotundi A., Bussoletti E., and Strazzulla G. (1997) Ultraviolet spectral changes in amorphous carbon grains induced by ion irradiation. *Astrophys. J., 481,* 545–549.

Mennella V., Brucato J. R., Colangeli L., and Palumbo P. (1999) Activation of the 3.4 micron band in carbon grains by exposure to atomic hydrogen. *Astrophys. J. Lett., 524,* L71–L74.

Mennella V., Muñoz C. G. M., Ruiterkamp R., Schutte W. A., Greenberg J. M., Brucato J. R., and Colangeli L. (2001) UV photodestruction of CH bonds and the evolution of the 3.4 μm feature carrier. II. The case of hydrogenated carbon grains. *Astron. Astrophys., 367,* 355–361.

Mishchenko M. I., Hovenier J. W., and Travis L. D. (2000) *Light Scattering by Nonspherical Particles: Theory, Measurements, and Applications.* Academic, San Diego. 690 pp.

Moore M. H. (1984) Studies of proton-irradiated SO_2 at low temperatures: Implications for Io. *Icarus, 59,* 114–128.

Moore M. H. and Hudson R. L. (1998) Infrared study of ion irradiated water ice mixtures with organics relevant to comets. *Icarus, 135,* 518–527.

Moore M. H. and Hudson R. L. (2000) IR detection of H_2O_2 at 80 K in ion-irradiated laboratory ices relevant to Europa. *Icarus, 145,* 282–288.

Moore M. H. and Hudson R. L. (2003) Infrared study of ion irradiated N_2-dominated ices relevant to Triton and Pluto: Formation of HCN and HNC. *Icarus, 161,* 486–500.

Mulas G., Baratta, G. A., Palumbo M. E., and Strazzulla G. (1998) Profile of CH_4 IR bands in ice mixtures. *Astron. Astrophys., 333,* 1025–1033.

Mumma, M. J. (1997) Organic volatiles in comets: Their relation to interstellar ices and solar nebula material. In *From Stardust to Planetesimals* (Y. J. Pendleton and A. G. G. M. Tielens, eds.), pp. 369–396. ASP Conference Series 122, Astronomical Society of the Pacific, San Francisco.

Mumma M. J., Blass W. E., Weaver H. A., and Larson H. P. (1988) Measurements of the ortho-para ratio and nuclear spin temperature of water vapor in comets Halley and Wilson (1986) and implications for their origin and evolution. *Bull. Am. Astron. Soc., 20,* 826.

Mumma M. J., DiSanti M. A., Dello Russo N., Fomenkova M., Magee-Sauer K., Kaminski C. D., and Xie D. X. (1996) Detection of abundant ethane and methane, along with carbon monoxide and water, in comet C/1996 B2 Hyakutake: Evidence for interstellar origin. *Science, 272,* 1310–1314.

Muñoz O., Volten H., de Haan J. F., Vassen W., and Hovenier J. W. (2000) Experimental determination of scattering matrices of olivine and Allende meteorite particles. *Astron. Astrophys., 360,* 777–788.

Notesco G. and Bar-Nun A. (1997) Trapping of methanol, hydrogen cyanide, and n-hexane in water ice, above its transformation temperature to the crystalline form. *Icarus, 126,* 336–341.

Notesco G. and Bar-Nun A. (2000) The effect of methanol clathrate hydrate formation and other gas-trapping mechanisms on the structure and dynamics of cometary ices. *Icarus, 148,* 456–463.

Notesco G., Bar-Nun A., and Owen T. (2003) Gas trapping in water ice at very low deposition rates and implication for comets. *Icarus, 162,* 183–189.

Nuth J. A., Hill H. G. M., and Kletetschka G. (2000) Determining the ages of comets from the fraction of crystalline dust. *Nature, 406,* 275–276.

Nuth J. A. III, Rietmeijer F. J. M., and Hill H. G. M. (2002) Condensation processes in astrophysical environments: The composition and structure of cometary grains. *Meteoritics & Planet. Sci., 37,* 1579–1590.

Owen T. and Bar-Nun A. (1993) Noble gases in atmospheres. *Nature, 361,* 693–694.

Owen T. and Bar-Nun A. (1995) Comets, impacts and atmospheres. *Icarus, 116,* 215–226.

Owen T., Bar-Nun A., and Kleinfeld I. (1991) Noble gases in

terrestrial planets: Evidence for cometary impacts? In *Comets in the Post-Halley Era I* (R. L. Newburn Jr. et al., eds.), pp. 429–437. Kluwer, Dordrecht.

Owen T., Bar-Nun A., and Kleinfeld I. (1992) Possible cometary origin of heavy noble gases in the atmospheres of Venus, Earth and Mars. *Nature, 358,* 43–46.

Palumbo M. E., Castorina A. C., and Strazzulla G. (1999) Ion irradiation effects on frozen methanol (CH_3OH). *Astron. Astrophys., 342,* 551–562.

Pendleton Y. J., Sandford S. A., Allamandola L. J., Tielens A. G. G. M., and Sellgren K. (1994) Near-infrared absorption spectroscopy of interstellar hydrocarbon grains. *Astrophys. J., 437,* 683–696.

Pepin R. O. (1997) Evolution of Earth's noble gases: Consequences of assuming hydrodynamic loss driven by giant impact. *Icarus, 126,* 148–156.

Prialnik D. and Bar-Nun A. (1992) Crystallization of amorphous ice as the cause of comet P/Halley's outburst at 14 AU. *Astron. Astrophys., 258,* L9–L12.

Richardson H. H., Wooldridge P. J., and Devlin J. P. (1985) FT-IR spectra of vacuum deposited clathrate hydrate of oxirane H_2S, THF, and ethane. *J. Chem. Phys., 83,* 4387–4394.

Rickman H. (1989) The nucleus of Comet Halley — surface structure, mean density, gas and dust production. *Adv. Space Res., 9,* 59–71.

Rietmeijer F. J. M. (1998) Interplanetary dust particles. In *Planetary Materials* (J. J. Papike, ed.), in *Rev. Mineral., 36,* pp. 2-1 to 2-95. Mineralogical Society of America, Washington, DC.

Rietmeijer F. J. M., Hallenbeck S. L., Nuth J. A. III, and Karner J. M. (2002) Amorphous magnesiosilicate smokes annealed in vacuum: The evolution of magnesium silicates in circumstellar and cometary dust. *Icarus, 156,* 269–286.

Rodgers S. D. and Charnley S. B. (2001) On the origin of HNC in comet Lee. *Mon. Not. R. Astron. Soc., 323,* 84–92.

Rotundi A., Brucato J. R., Colangeli L., Ferrini G., Mennella V. E., and Palumbo P. (2002) Production, processing and characterisation techniques for cosmic dust analogues. *Meteoritics & Planet. Sci., 37,* 1623–1635.

Salama F., Allamandola L. J., Witteborn F. C., Cruikshank D. P., Sandford S. A., and Bregman J. D. (1990) The 2.5–5.0 micron spectra of Io — Evidence for H_2S and H_2O frozen in SO_2. *Icarus, 83,* 66–82.

Sandford S. A. and Allamandola L. J. (1988) The condensation and vaporization behavior of H_2O : CO ices and implications for interstellar grains and cometary activity. *Icarus, 76,* 201–224.

Schmitt B. and Klinger J. (1987) Different trapping mechanisms of gases by water ice and their relevance for comet nuclei. In *The Diversity and Similarity of Comets* (E. J. Rolfe et al., eds.), pp. 613–619. ESA SP-278, Noordwijk, The Netherlands.

Schmitt B., Espinasse S., Grim R. J. A., Greenberg J. M., and Klinger J. (1989a) Laboratory studies of cometary ice analogues. In *Proceedings of an International Workshop on Physics and Mechanics of Cometary Materials* (J. Hunt and T. D. Guyenne, eds.), pp. 65–69. ESA SP-302, Noordwijk, The Netherlands.

Schmitt B., Greenberg J. M., and Grim R. J. A. (1989b) The temperature dependence of the CO infrared band strength in CO : H_2O ices. *Astrophys. J. Lett., 340,* L33–L36.

Seiferlin K., Komle N. I., Kargl G., and Spohn T. (1996) Line heat source measurements of the thermal conductivity of porous H_2O ice, CO_2 ice and mineral powders under space conditions. *Planet. Space. Sci., 44,* 691–704.

Spohn T., Seiferlin K., and Benkhoff J. (1989) Thermal conductivities and diffusivities of porous ice samples at low pressures and temperatures and possible modes of heat transfer in near surface layers of comets. In *Proceedings of an International Workshop on Physics and Mechanics of Cometary Materials* (J. Hunt and T. D. Guyenne, eds.), pp. 77–81. ESA SP-302, Noordwijk, The Netherlands.

Strazzulla G. and Johnson R. E. (1991) Irradiation effects on comets and cometary debris. In *Comets in the Post-Halley Era* (R. Newburn Jr et al., eds.), pp. 243–275. Kluwer, Dordrecht.

Strazzulla G. and Palumbo M. E. (1998) Evolution of icy surfaces: an experimental approach. *Planet. Space Sci., 46,* 1339–1348.

Strazzulla G. and Palumbo M. E. (2001) Organics produced by ion irradiation of ices: Some recent results. *Adv. Space Res., 27,* 237–243.

Strazzulla G., Baratta G. A., and Palumbo M. E. (2001) Vibrational spectroscopy of ion-irradiated ices. *Spectrochim. Acta, 57A,* 825–842.

Thompson S. P., Evans A., and Jones A. P. (1996) Structural evolution in thermally processed silicates. *Astron. Astrophys., 308,* 309–320.

van de Hulst H. C. (1957) *Light Scattering by Small Particles.* Wiley, New York. 470 pp.

Volten H., Muñoz O., Rol E., de Haan J. F., Vassen W., Hovenier J. W., Muinonen K., and Nousiainen T. (2001) Scattering matrices of mineral aerosol particles at 441.6 nm and 632.8 nm. *J. Geophys. Res., 106,* 17375–17402.

Weidenschilling S. (1997) The origin of comets in the solar nebula: A unified model. *Icarus, 127,* 290–306.

Weissman P. R. (1986) Are cometary nuclei primordial rubble piles? *Nature, 320,* 242–244.

Weissman P. R., Asphaug E., and Lowry S. C. (2004) Structure and density of cometary nuclei. In *Comets II* (M. C. Festou et al., eds.), this volume. Univ. of Arizona, Tucson.

Wilkening L., ed. (1982) *Comets*. Univ. of Arizona, Tucson. 775 pp.

Wooden D. H., Harker D. E., Woodward C. E., Butner H. M., Koike C., Witteborn F. C., and McMurtry C. W. (1999) Silicate mineralogy of the dust in the inner coma of comet C/1995 O1 (Hale-Bopp) pre- and postperihelion. *Astrophys. J., 517,* 1034–1058.

Wopenka B. (1988) Raman observations on individual interplanetary dust particles. *Earth Planet. Sci. Lett., 88,* 221–231.

Wu C. Y. R., Judge D. L., Cheng B.-M., Shih W. H., Yih T. S., and Ip W. H. (2002) Extreme ultraviolet photon-induced chemical reactions in the C_2H_2-H_2O mixed ices at 10 K. *Icarus, 156,* 456–473.

Wu C. Y. R., Judge D. L., Cheng B.-M., Yih T.-S., Lee C. S., and Ip W. H. (2003) Extreme ultraviolet photolysis of CO_2-H_2O mixed ices at 10 K. *J. Geophys. Res., 108(E4),* 13-1 to 13-8.